Robust Beamforming Optimization for Self-Sustainable Intelligent Reflecting Surface Assisted Wireless Networks

Journal:	*IEEE Transactions on Cognitive Communications and Networking*
Manuscript ID	TCCN-TPS-21-0147.R1
Manuscript Type:	Transactions Paper Submissions
Date Submitted by the Author:	06-Oct-2021

Complete List of Authors:	Zou, Yuze; Huazhong University of Science and Technology, School of Electronic Information and Communications Long, Yusi; Guangzhou University, School of Electronics and Communication Engineering Gong, Shimin; Sun Yat-Sen University, Dinh , Hoang; University of Technology Sydney Faculty of Engineering and Information Technology, School of Electrical and Data Engineering Liu, Wei; Huazhong University of Science and Technology, School of Electronic Information and Communications Niyato, Dusit; Nanyang Technological University, Cheng, Wenqing ; Huazhong University of Science and Technology, School of Electronic Information and Communications

Keyword:	

Robust Beamforming Optimization for Self-Sustainable Intelligent Reflecting Surface Assisted Wireless Networks

Yuze Zou, Yusi Long, Shimin Gong, Dinh Thai Hoang, Wei Liu, Wenqing Cheng, and Dusit Niyato

***Abstract*—We focus on an intelligent reflecting surface (IRS)-assisted multiple-input single-output (MISO) system where the IRS sustains its operations by harvesting energy from the access point (AP) in the power splitting (PS) protocol. We aim to minimize the AP's transmit power subject to the receivers' signal-to-noise ratio (SNR) and the IRS's energy budget constraints. A two-stage optimization framework is proposed to jointly optimize the AP's active beamforming, the IRS's passive beamforming, and the reflection amplitude. Given the reflection amplitude, we employ alternating optimization to update the beamforming strategies. Then, we determine the lower and upper bounds of the reflection amplitude in closed-form expressions, which help to update the reflection amplitude in a bisection method. We further extend our study to the robust case with uncertain channels. Our analysis reveals that the robust counterpart can be solved by the same optimization framework. Extensive simulations reveal that our algorithm is efficacy to balance the IRS's energy budget and the receiver's SNR performance. With uncertain channel information, a larger size of the IRS does not always ensure a higher performance improvement to information transmissions.**

***Index Terms*—Energy harvesting, intelligent reflecting surface, robust optimization, passive beamforming**

I. Introduction

Recently, the intelligent reflecting surface (IRS) has been proposed as a promising technology to improve the energy- and spectrum-efficiency of wireless communications by adaptively configuring the signal propagation conditions [1]. The IRS is composed of a large array of low-cost and passive scattering elements with specially designed physical dimensions. Each element is controllable by an embedded controller chip and used to induce a phase shift to the incident RF signals [2]. By a joint control of the phase shifts of all scattering elements, namely, passive beamforming, the reflected signals can create preferable channel conditions for information transmissions. This implies an additional degree of freedom for the design and optimization of wireless networks. Hence, it is envisioned as a revolutionary technology to integrate the online configurable IRS into the future wireless networks [3]–[5]. Extensive surveys in [1] and [2] have revealed that the joint optimization of the IRS's passive beamforming and the RF radios' active beamforming can significantly improve the network performance by playing different roles such as the signal reflector, transmitter, and even the receiver. The performance improvement of IRS-assisted networks has been investigated in a wide range of applications, such as mobile edge computing [6], [7], wireless powered communication networks [8]–[10], and secure wireless transmission [11]–[13].

Typically, the IRS is assumed to be an ideal passive device with negligible energy consumption. This capability ensures its wide deployment in outdoor environments, e.g., the facts of buildings and moving vehicles. For example, the authors in [8] investigated an IRS-assisted wireless powered sensor network where a group of sensors can harvest RF energy from a power station and operate in the harvest-then-transmit protocol. A sum throughput maximum problem is formulated by jointly optimizing the IRS's phase shifts and the users' time allocations. In fact, the IRS's energy consumption depends on its physical dimensions and the implementation of its scattering elements. The authors in [14] proposed a linear model to describe the IRS's energy consumption, which is proportionally increasing with the number of scattering elements. Moreover, the energy consumption of each scattering element depends on its phase resolution, i.e., a finer tuning of the phase shifts implies a higher energy consumption of each scattering element due to more complicated circuit design. As the size of IRS increases, its energy consumption is no longer negligible and becomes a critical design aspect for overall performance improvement. However, how to fulfill the IRS's energy demand still remains as an open problem.

Another common assumption in the literature is that the joint active and passive beamforming optimization is performed based on perfect channel state information (CSI). However, it is challenging to obtain the accurate CSI of the AP-IRS channel and IRS-user channel in practice due to the fact that the reflective elements at the IRS are passive and have limited signal processing capabilities. Specifically, there are two typical IRS-related channel estimation approaches. One is to estimate AP-IRS and IRS-user channels separately [15] and the other is to estimate the cascaded AP-IRS-user channel [16]–[18]. For both approaches, the channel estimation error

Yuze Zou is with the School of Electronic Information and Communications, Huazhong University of Science and Technology, China (e-mail: zouyuze@hust.edu.cn). Yusi Long is with the School of Intelligent Systems Engineering, Sun Yat-sen University, China (longys@mail2.sysu.edu.cn). Shimin Gong is with the School of Intelligent Systems Engineering, Sun Yat-sen University, China (e-mail: gongshm5@mail.sysu.edu.cn). Dinh Thai Hoang is with the Department of Electrical and Data Engineering, University of Technology Sydney, Australia (e-mail: hoang.dinh@uts.edu.au). Wei Liu is with the School of Electronic Information and Communications, Huazhong University of Science and Technology, China (e-mail: liuwei@hust.edu.cn). Wenqing Cheng is with the School of Electronic Information and Communications, Huazhong University of Science and Technology, China (e-mail: chengwq@hust.edu.cn). Dusit Niyato is with the School of Computer Science and Engineering, Nanyang Technological University, Singapore (e-mail: dniyato@ntu.edu.sg).

is inevitable due to processing delay and limited sampling rate in a dynamic channel environment [18]–[20]. The joint active and passive beamforming optimization may face severe performance loss if countermeasures are not taken properly against the channel uncertainty. For example, the authors in [21] revealed that the phase error in channel estimation may bring the ambiguity in the IRS's phase tuning. Thus, it is practical to quantize the channel uncertainty and design robust control strategy to countermeasure the uncertainty. To fight against the channel uncertainty, the authors in [22] modeled the error estimates as Gaussian variables and studied the asymptotical performance loss of spectrum efficiency in IRS-assisted uplink transmissions. Instead of the stochastic approach in [22], another approach for modeling the channel uncertainty is to impose a bounded norm on the error estimates. This normally results in a robust formulation to ensure the worst-case performance guarantee. For example, considering the norm-based uncertainty model for the channels from the IRS to the receivers, a robust power minimization problem was studied in [18] subject to the worst-case data rate requirements at individual receivers. The authors in [20] assumed that the cascaded channel from the base station to the receiver via the IRS is subject to a norm-based uncertainty model. A similar model was applied in [23] to improve the IRS-assisted secure communication performance, where a robust sum-rate maximization problem was studied subject to the worst-case information leakage to an eavesdropper. The solutions to the above robust problems typically rely on convex reformulations of the worst-case constraints, and then use the alternating optimization (AO) method to optimize the joint beamforming strategies iteratively.

In this paper, we address the above-mentioned difficulties in an IRS-assisted wireless system considering the IRS's self-sustainability and channel uncertainties. In particular, we envision a multi-input single-output (MISO) downlink system from a multi-antenna access point (AP) to single-antenna receivers assisted by the IRS. The IRS is self-sustainable by harvesting RF energy from the AP's active beamforming. To sustain its operations, the IRS is capable of controlling its reflection amplitude flexibly such that a part of the incident RF signals is reflected while the other part is harvested as energy. The control of the IRS's reflection amplitude is similar to the conventional power splitting (PS) protocol for energy harvesting devices [24]. The self-sustainable IRS was also studied in our previous work [25], where the time switching (TS) protocol was considered for the IRS to transit between energy harvesting and IRS-assisted information transmissions. Similarly, the authors in [26] proposed the IRS-assisted harvest-then-transmit time switching transmission policy for the wireless sensor network. To fulfill the IRS's energy demand, the IRS is allocated with a dedicated time slot to harvest RF energy from the power station. Different from the TS protocol in [25] and [26], we consider the PS protocol for the IRS to harvest RF energy and sustain its operation, which provides another self-sustainable design for the IRS-assisted MISO system. In [27], the authors investigated both the TS and PS protocols for self-sustainable IRS-assisted wireless powered communication networks. Different from [27] and [26], we jointly optimize active beamforming at the AP and passive beamforming at the IRS and its reflection amplitude to assist the MISO system sustainably in PS protocol. Moreover, a practical case with imperfect CSI is considered and we employ the norm-based uncertainty model to characterize the cascaded channel from the AP to receivers, which is the product of the AP-IRS and IRS-user channels. Different from [18], [20], [22], [23], we focus on a more practical case with both the worst-case SNR requirements at the receivers and the worst-case power budget constraint at the IRS.

Some preliminary results on the robust beamforming optimization were previously presented in our conference paper [28]. In this paper, we present a comprehensive analysis and unified solution for both the non-robust and robust cases. In particular, we firstly formulate an optimization problem to minimize the AP's transmit power by jointly optimizing the AP's active beamforming and the IRS's passive beamforming strategies with perfect CSI. Then, the problem is extended to its robust counterpart under imperfect CSI. It is clear that the AP's active beamforming not only determines the data rate to the information receiver, but also affects the energy harvesting capability at the IRS. This implies a close coupling between the AP's active beamforming and the IRS's optimal control on its phase shifting matrix and the reflection coefficient. By exploiting the problem structure, we decompose the optimization of the IRS's phase shifting matrix and the reflection coefficient into two sub-problems, i.e., the inner-loop and outer-loop optimizations in an iterative manner. Given the outer-loop reflection coefficient, the inner-loop joint beamforming optimization follows the conventional AO method. Then, the IRS's reflection coefficient in the outer loop can be updated in a closed-form expression. Most importantly, this method provides a generalized optimization framework for both the non-robust and robust cases. For clarification, we summarize our main contributions in this paper as follows.

- Firstly, we focus on a generic MISO system assisted by a self-sustainable IRS, which has been seldom studied in the literature. The AP's active beamforming and the IRS's passive beamforming and its reflection amplitude are jointly optimized to assist the MISO downlink transmissions in the PS protocol. We believe that our work provide necessary supplement to the current literatures by considering IRS's self-sustainability and its practical deployments with uncertain channel conditions.
- Secondly, we consider imperfect channel state information due to the inevitable estimation error in the IRS-related channels, incurred by the passive nature of the IRS. We provide a unified solution framework for both robust and non-robust cases. Specifically, by exploiting the problem structure, a two-stage algorithm is devised to jointly optimize the AP's active beamforming, the IRS's passive beamforming and the reflection amplitude. A closed-form update for reflection amplitude is derived under the perfect channel state information and its update for the robust counterpart is also proposed.
- Thirdly, we perform intensive simulations to show the performance impacts of the IRS's deployment parame-

TABLE I: Math Notations and Operators

Notations	Definitions
$\|\cdot\|$	Euclidean norm of a complex vector
$\|\cdot\|$	Modulus of a complex number
$(\cdot)^T$	Transpose operator
$(\cdot)^H$	Conjugate transpose operator
$\mathbb{C}^{a\times b}$	Space of complex matrices with size $a \times b$
$\mathbf{I}_M$	Identity matrix with size M
$\mathrm{Re}\,(\cdot)$	Real part of a complex number
$\mathrm{vec}(\cdot)$	Vectorization of a matrix variable
$\arg(\mathbf{a})$	Angle vector of elements in vector $\mathbf{a}$
$\otimes$	Kronecker product of matrices
$\mathrm{Tr}(\mathbf{X})$	Trace of matrix $\mathbf{X}$
$\mathrm{diag}(\mathbf{a})$	Diagonal matrix with the diagonal vector $\mathbf{a}$
$\mathbf{A} \succeq 0$	$\mathbf{A}$ is a positive semidefinite matrix

ters under both non-robust and robust conditions. These results reveal some important information in designing the IRS-assisted MISO systems. For example: 1) The proposed algorithm is shown to be efficient to balance the IRS's energy budget and the receiver's signal enhancement by tuning IRS's reflection amplitude. 2) With imperfect channel state information, a larger size of the IRS does not always ensure a higher performance improvement to the information transmission between the AP and the user. 3) For practical considerations, the IRS's discrete phase shifting is also analyzed and evaluated via simulations. With 3-bit phase resolution, the discrete phase shifting scheme can achieve nearly the optimal performance of the ideal continuous phase shifting scheme.

The remainder of the paper is organized as follows. We present the system model in Section II, and propose the algorithm to minimize the AP's transmit power with perfect CSI in Section III. Then, we derive the robust counterpart and its reformulation with norm-based channel uncertainties in Section IV. Numerical results are presented in Section V and conclusions are summarized in Section VI. Some operators and notations used in this paper are listed in Table I for clarity.

II. System model

We consider a MISO wireless downlink communication system assisted by an IRS with N elements as illustrated in Fig. 1. The AP with M antennas serves multiple receivers equipped with a single antenna. To avoid interference, we assume that each receiver is allocated an orthogonal channel for information transmission, e.g., by using the time division multiple access (TDMA) scheme. Multiple receivers can be also served simultaneously by the multi-antenna AP. In this case, the AP's transmit precoding has to be properly designed to mitigate the interference among different receivers. More importantly, we can verify that our solution method proposed for TDMA scheme can be easily extended to this multi-user case with minor revisions, e.g., [5], [9]. Without loss of generality, we focus on the TDMA scheme in the following part and formulate our design problem in each time slot with a single receiver. The IRS controller is capable of adjusting the phase shift of each reflecting element dynamically according to the CSI. The joint control of phase shifts, namely, passive beamforming, provides the capability of shaping the physical channel as desired. The AP-receiver, AP-IRS, and IRS-receiver channels are denoted by $\mathbf{g} \in \mathbb{C}^{M\times 1}$, $\mathbf{H} \in \mathbb{C}^{M\times N}$ and $\mathbf{f} \in \mathbb{C}^{N\times 1}$, respectively. The channel estimation can follow a similar approach as that in [29]. The RF transmitter firstly sends pilot signals to the receiver. Meanwhile, the receiver or IRS can estimate the corresponding AP-receiver or IRS-receiver channels. Then, the AP can jointly optimize its active beamforming, the IRS's phase shifting matrix and the reflection amplitude, which can be distributed to the IRS at the beginning of each time slot for information transmission.

A. IRS-assisted Channel Enhancement

Besides phase tuning, we also assume that the IRS controller can adjust the magnitude of its reflecting coefficients. Similar to backscatter communications, each reflecting element sets a phase shift $\theta_n \in [0, 2\pi)$[1] and its magnitude $\rho_n \in [0, 1]$ to reflect the incident RF signals. Let $\mathbf{\Theta} = \mathrm{diag}(\rho_1 e^{j\theta_1}, \ldots, \rho_N e^{j\theta_N})$ denote the IRS's passive beamforming strategy. Hence, the IRS-assisted equivalent channel from the AP to the receiver is given by

$$\hat{\mathbf{g}} = \mathbf{g} + \mathbf{H}\mathbf{\Theta}\mathbf{f}, \tag{1}$$

where $\mathbf{H} = [\mathbf{h}_1, \ldots, \mathbf{h}_N]$ denotes the channel from the AP to the IRS. We can also define the IRS-assisted reflecting channel $\mathbf{H_f}$ from the AP to the receiver as follows:

$$\mathbf{H_f} \triangleq \mathbf{H}\mathrm{diag}(\mathbf{f}) = [f_1\mathbf{h}_1, f_2\mathbf{h}_2, \ldots, f_N\mathbf{h}_N]. \tag{2}$$

Hence, the channel model in (1) can be equivalently rewritten as $\hat{\mathbf{g}} = \mathbf{g} + \mathbf{H_f}\mathbf{v}$ where $\mathbf{v} = [\rho_1 e^{j\theta_1}, \ldots, \rho_N e^{j\theta_N})]^T$ denotes the diagonal vector of the matrix $\mathbf{\Theta}$. We consider linear beamforming at the AP, with $\mathbf{w} \in \mathbb{C}^{M\times 1}$ denoting the transmit beamforming vector. Let s denote the complex symbol with unit transmit power. The received signal at the receiver is given by $y = \hat{\mathbf{g}}^H\mathbf{w}s + \nu_d$, where ν_d is the additive white Gaussian noise at the receiver. Without loss of generality, we can normalize the noise variance to unit one. Therefore, the SNR at the receiver can be characterized as $\gamma(\mathbf{w}, \mathbf{\Theta}) = \|(\mathbf{g} + \mathbf{H}\mathbf{\Theta}\mathbf{f})^H\mathbf{w}\|^2$.

B. IRS's Power Budget Constraint

Given the AP's transmit beamforming, the incident signal at the IRS is $\mathbf{x} = \mathbf{H}^H\mathbf{w}s$. We assume that each tunable chip of the reflecting element is also equipped with an energy harvester circuit that is able to harvest RF energy from the AP's beamforming signals. In particular, the IRS's energy harvesting follows a similar PS protocol as that of the conventional wireless powered relay communications [24]. For the n-th reflecting element of the IRS, by tuning the reflection

[1]Practically, phase shifts can be selected from a finite set for the ease of implementation. Given the continuous phase shifts, the discrete phase shifts can be obtained by quantization projection, e.g., [8], [30].

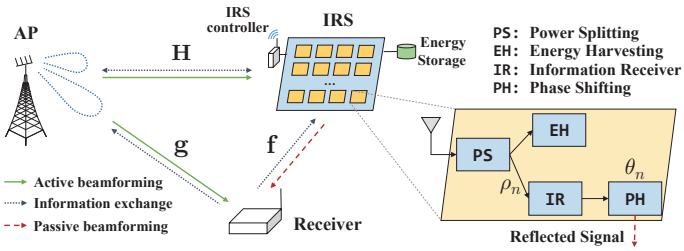

Fig. 1: The IRS-assisted MISO system model in the PS protocol.

amplitude ρ_n, part of the incident signal is reflected to the receiver (denoted by $\rho_n \mathbf{h}_n^H \mathbf{w} s$), while the remaining part is fed to the energy harvester. Hence, the parameter ρ_n^2 can be regarded as the power splitting (PS) ratio [2]. The amplitude adjusting can be achieved by using electronic devices such as positive-intrinsic-negative (PIN) diodes, field-effect transistors (FET), micro-electromechanical system (MEMS) switches, and variable resistor loads, e.g., [5], [31]. A similar PS protocol for self-sustainable IRS-assisted system is discussed in [27].

We consider a linear power consumption model as that in [14], where the IRS's power consumption is linearly proportional to the number of reflecting elements and the phase resolution of each scattering element. To maintain the IRS's operations, the total harvested energy has to meet the IRS's total power consumption. Besides, a linear energy harvesting (EH) model is considered as well. We further assume a simplified case that all the IRS's reflecting elements set the same reflection amplitude [3], i.e., $\rho_1 = \cdots = \rho_N = \rho$. Then, we can rewrite the equivalent channel as $\hat{\mathbf{g}} = \mathbf{g} + \rho \mathbf{H}_\mathbf{f} \boldsymbol{\theta}$, where $\boldsymbol{\theta} = [e^{j\theta_1}, \ldots, e^{j\theta_N}]^T$. The IRS's energy budget constraint can be given as $\eta \sum_n \left(1 - \rho_n^2\right) |\mathbf{h}_n^H \mathbf{w}|^2 = \eta \left(1 - \rho^2\right) \|\mathbf{H}^H \mathbf{w}\|^2 \geq N\mu$, where η represents the energy harvesting coefficient and $\mathbf{h}_n$ denotes the channel vector from the AP to the n-th reflecting element. We further assume that the phase resolutions of the IRS's scattering elements are identical [14]. Hence, the IRS's power consumption is given by $N\mu$, where μ denotes the power consumption of each scattering element.

Focusing on information transmission in one specific time slot, we aim to minimize the AP's transmit power, denoted as $\|\mathbf{w}\|^2$, by jointly optimizing the active and passive beamforming strategies, constrained by the IRS's power budget and the receiver's SNR requirements.

$$\min_{\mathbf{w},\boldsymbol{\theta},\rho} \quad \|\mathbf{w}\|^2, \tag{3a}$$

$$\text{s.t.} \quad |(\mathbf{g} + \rho \mathbf{H}_\mathbf{f} \boldsymbol{\theta})^H \mathbf{w}|^2 \geq \gamma_0, \tag{3b}$$

$$\eta(1 - \rho^2) \|\mathbf{H}^H \mathbf{w}\|^2 \geq N\mu, \tag{3c}$$

$$\rho \in [0, 1] \text{ and } \theta_n \in [0, 2\pi) \quad \forall n \in \mathcal{N}. \tag{3d}$$

Note that (3c) denotes a linear EH model for simplicity. In fact, a more practical non-linear EH model can be also applied here [32]. Denote the non-linear EH model as $f(P)$, where P is the input power. Considering the concave and non-decreasing properties of $f(P)$, we can verify that the proposed solution method for linear EH model is still applicable to the non-linear EH model with minor modification. Given the non-linear EH model, we can simply retrieve the IRS's power demand as $f^{-1}(N\mu)$, where $f^{-1}(\cdot)$ is the reverse function of $f(\cdot)$ and denotes a constant given the size of the IRS. It is clear that the solution to problem (3) relies on the channel information. In the following, we firstly consider the case with perfect CSI and propose the joint beamforming optimization solution to minimize the AP's transmit power. Then, a robust counter-part of problem (3) can be reformulated by considering an analytical model for channel uncertainties. We envision that the solution to the non-robust case can shed some insights on the algorithm design for a more practical case with uncertain CSI.

III. Transmit Power Minimization with Perfect CSI

With known CSI, the non-convex problem (3) can be solved by the general AO algorithm. In particular, we can solve each set of variables, i.e., $\boldsymbol{\theta}$, $\mathbf{w}$ or ρ, sequentially and iteratively while the other variables are fixed. For any fixed ρ in the outer loop, the inner-loop optimization of the active and passive beamforming $(\mathbf{w}, \boldsymbol{\theta})$ can follow a similar semidefinite relaxation (SDR) method as that of [33]. Given the active beamforming $\mathbf{w}$, the constraints (3b)-(3c) define the lower and upper bounds on ρ. This implies that we can use a linear search method to update the reflection amplitude ρ in the outer loop.

Before we dive into the algorithm design, it is necessary to check the feasibility of problem (3), which helps us build a feasible region for the iterative search algorithm. Intuitively, we can always find a sufficiently large transmit power $\|\mathbf{w}\|^2$ to ensure the fulfillment of both the SNR and power budget constraints in (3). This implies that we can set the upper bound on the AP's transmit power as $\|\mathbf{w}\|_{\max}^2 \triangleq \gamma_0 / \|\mathbf{g}\|^2$ according to the SNR constraint (3b), by assuming that there is no assistance from the IRS. If the solution to problem (3) exceeds $\|\mathbf{w}\|_{\max}^2$, this means that a significant portion of the AP's transmit power will be used to maintain the IRS's self-sustainability. In this case, there is no need to use the IRS to assist the AP's information transmission. Based on the IRS's power budget constraint (3c), it is easy to find the AP's minimum transmit power by the following problem:

$$\|\mathbf{w}\|_{\min}^2 \triangleq \arg\min_{\mathbf{w}} \left\{ \|\mathbf{w}\|^2 \;\middle|\; \|\mathbf{H}^H \mathbf{w}\|^2 \geq N\mu/\eta \right\}, \tag{4}$$

which can be solved by adopting the SDR technique to convert it into a semidefinite program (SDP). Then, problem (3) becomes infeasible if the solution is smaller than $\|\mathbf{w}\|_{\min}^2$. To ensure the feasibility of problem (3), we thus require the non-trivial condition $\|\mathbf{w}\|_{\min}^2 < \|\mathbf{w}\|_{\max}^2$. This condition also ensures that the use of IRS can provide better performance than that of the non-IRS-assisted system. In the following part, we firstly provide the AO method to optimize the joint beamforming strategies $(\mathbf{w}, \boldsymbol{\theta})$ with a fixed reflection amplitude ρ. After that, with the fixed $(\mathbf{w}, \boldsymbol{\theta})$, a search method is devised to update ρ by exploiting the problem's structural property.

[2] Without abuse of notation, the PS ratio and reflection amplitude are used interchangeably in the rest of this paper.

[3] For ease of implementation, it is reasonable to simplify the circuit design and reduce the circuit's power consumption by setting all amplitude reflections to be the same, similar to that in [27].

A. Inner-loop Beamforming Optimization

With the fixed ρ in problem (3), we decompose the optimization of $(\mathbf{w}, \boldsymbol{\theta})$ in two steps. Firstly, we optimize the IRS's phase vector $\boldsymbol{\theta}$ to maximize the channel gain of the cascaded channel as shown in (3b). Secondly, once we obtain $\boldsymbol{\theta}$, the active beamforming $\mathbf{w}$ can be optimized by formulating problem (3) into an SDP, which can be efficiently solved by the interior-point method [34]. In the first step, the optimization of $\boldsymbol{\theta}$ is simply given as follows:

$$\max_{\boldsymbol{\theta}} \quad |(\mathbf{g} + \rho \mathbf{H_f} \boldsymbol{\theta})^H \mathbf{w}|^2, \quad \text{s.t.}\, \theta_n \in [0, 2\pi),\ \forall n \in \mathcal{N}. \quad (5)$$

Let $\bar{\boldsymbol{\theta}} = [\boldsymbol{\theta}, \zeta]^T = [e^{j\theta_1}, \ldots, e^{j\theta_N}, \zeta]^T$ where ζ is an auxiliary variable such that $\zeta \geq 0$ and $|\zeta| = 1$. The objective in (5) can be expanded and rewritten in a compact form as $\bar{\boldsymbol{\theta}}^H \mathbf{R} \bar{\boldsymbol{\theta}}$, where the matrix coefficient $\mathbf{R}$ is given by $\mathbf{R} = \begin{bmatrix} \rho^2 \mathbf{H_f}^H \mathbf{w}\mathbf{w}^H \mathbf{H_f} & \rho \mathbf{H_f}^H \mathbf{w}\mathbf{w}^H \mathbf{g} \\ \rho \mathbf{g}^H \mathbf{w}\mathbf{w}^H \mathbf{H_f} & 0 \end{bmatrix}$. We further apply SDR to the quadratic term $\bar{\boldsymbol{\theta}}^H \mathbf{R} \bar{\boldsymbol{\theta}}$ by introducing a rank-one matrix $\bar{\boldsymbol{\Theta}}$. As such, problem (5) can be converted into an SDP as follows, similar to that in [35] and [36].

$$\max_{\bar{\boldsymbol{\Theta}} \succeq 0} \quad \mathrm{Tr}(\mathbf{R}\bar{\boldsymbol{\Theta}}), \quad \text{s.t.}\, \bar{\boldsymbol{\Theta}}_{n,n} = 1, \quad \forall n = 1, \ldots, N+1, \quad (6)$$

which can be solved efficiently by the off-the-shelf solver [37]. In the second step, with the fixed $\boldsymbol{\theta}$, the optimization of $\mathbf{w}$ in problem (3) can be reformulated into an SDP as follows:

$$\min_{\mathbf{W} \succeq 0} \quad \mathrm{Tr}(\mathbf{W}), \quad (7a)$$

$$\text{s.t.} \quad \mathrm{Tr}(\hat{\mathbf{G}}\mathbf{W}) \geq \gamma_0, \quad (7b)$$

$$\mathrm{Tr}(\mathbf{H}\mathbf{H}^H \mathbf{W}) \geq N\mu\eta^{-1}(1-\rho^2)^{-1}, \quad (7c)$$

where $\hat{\mathbf{G}} = \hat{\mathbf{g}}\hat{\mathbf{g}}^H$ denotes the equivalent channel matrix from the AP to the receiver, and $\mathbf{W}$ is the SDR of the quadratic term $\mathbf{w}\mathbf{w}^H$, i.e., $\mathbf{W} \succeq \mathbf{w}\mathbf{w}^H$. Given ρ and $\boldsymbol{\theta}$, the channel matrix $\hat{\mathbf{G}}$ becomes constant in problem (7). Hence, problem (7) has a similar structure as that of problem (6). Both of them can be efficiently solved by the interior-point method. Generally, the relaxed problems (6) and (7) may not lead to a rank-one solution. This implies that the optimal objective value of problem (6) only provides an upper bound of problem (5). Similarly, the optimal solution in (7) can be considered as a lower bound on the optimization of active beamforming in the second step. As such, additional steps are required to construct a rank-one solution to the problem (5) from the optimal high-rank solution to the problem (6). Similarly, the rank-one beamforming vector $\mathbf{w}$ also needs to be extracted from the optimal solution $\mathbf{W}$ to the problem (7).

Gaussian randomization method (GRM) is one of the efficient methods to construct rank-one solutions from the optimal solutions to SDR problems [38]. Specifically, for passive beamforming in (6), we can firstly obtain the eigenvalue decomposition as $\bar{\boldsymbol{\Theta}} = \mathbf{U}\boldsymbol{\Sigma}\mathbf{U}^H$, where $\mathbf{U} = [\mathbf{e}_1, \ldots, \mathbf{e}_{N+1}]$ and $\boldsymbol{\Sigma} = \mathrm{diag}(\lambda_1, \ldots, \lambda_{N+1})$ are a unitary matrix and a diagonal matrix, respectively, both with the size of $(N+1) \times (N+1)$. Then, we can construct a suboptimal solution to problem (5) as $\bar{\boldsymbol{\theta}} = \mathbf{U}\sqrt{\boldsymbol{\Sigma}}\mathbf{r}$, where $\mathbf{r} \in \mathcal{CN}(\mathbf{0}, \mathbf{I}_{N+1})$ is a random vector generated from the circularly symmetric complex Gaussian distribution with zero mean and the covariance matrix $\mathbf{I}_{N+1}$. Given a set of randomly generated Gaussian vectors $\mathbf{r}$, we find the best $\bar{\boldsymbol{\theta}}$ (denoted by $\bar{\boldsymbol{\theta}}^*$) that maximizes the objective value in (5). Finally, the approximate solution to problem (5) can be recovered by $\boldsymbol{\theta} = e^{j \arg([\bar{\boldsymbol{\theta}}^* / \bar{\theta}^*_{N+1}]_{(1:N)})}$, where $[\boldsymbol{x}]_{(1:N)}$ denotes the vector of the first N elements in $\boldsymbol{x}$ [35]. It has been shown that a sufficiently large number of the randomly generated vectors $\mathbf{r}$ can be used to generate a good approximation of problem (5) [38]. The same procedures can be applied to problem (7) can then used to retrieve the rank-one approximate solution $\mathbf{w}$.

Algorithm 1 Two-stage Beamforming Optimization with Perfect CSI

1: $\|\mathbf{w}^{(0)}\|^2 \leftarrow +\infty$, $k \leftarrow 1$, $\epsilon \leftarrow 10^{-5}$
2: Initialize $\boldsymbol{\theta}$ randomly, $\mathbf{w}^{(k)} \leftarrow \|\mathbf{w}\|^2_{\max}$
3: Evaluate $\rho^{(k)}_{\min}$, $\rho^{(k)}_{\max}$, and initialize $\rho^{(k)} \in (\rho^{(k)}_{\min}, \rho^{(k)}_{\max})$
4: **while** $|\|\mathbf{w}^{(k)}\|^2 - \|\mathbf{w}^{(k-1)}\|^2| > \epsilon$
5: $\quad k \leftarrow k + 1$
6: $\quad$ **Inner-loop update** $(\boldsymbol{\theta}, \mathbf{w})$
7: $\quad\quad$ **Update** $\boldsymbol{\theta}$: solve (6) to retrieve $\boldsymbol{\theta}$
8: $\quad\quad$ **Update** $\mathbf{w}^{(k)}$: solve (7) to retrieve $\mathbf{w}$, $\mathbf{w}^{(k)} \leftarrow \mathbf{w}$
9: $\quad$ **Outer-loop update** $(\rho^{(k)}_{\min}, \rho^{(k)}_{\max})$ by Proposition 2
10: $\quad\quad \rho^{(k)} \leftarrow (\rho^{(k)}_{\min} + \rho^{(k)}_{\max})/2$
11: **end while**

Besides the AO method to optimize $(\mathbf{w}, \boldsymbol{\theta})$, we also propose a heuristic method to simplify the computation and reduce the number of iterations. Note that the IRS's phase vector $\boldsymbol{\theta}$ only appears in the constraint (3b). The use of IRS can be simply set to enhance the equivalent channel gain $\|\mathbf{g} + \rho \mathbf{H_f} \boldsymbol{\theta}\|^2$ by tuning its phase vector $\boldsymbol{\theta}$, regardless of the AP's active beamforming $\mathbf{w}$. Hence, we call this heuristic method as the Max-Gain algorithm. Given the receiver's SNR requirement, the channel enhancement in return can reduce the AP's transmit power. By this intuition, the IRS's phase vector $\boldsymbol{\theta}$ becomes the solution to the following problem:

$$\max_{\boldsymbol{\theta}} \quad \|\mathbf{g} + \rho \mathbf{H_f} \boldsymbol{\theta}\|^2, \quad \text{s.t.} \quad \theta_n \in [0, 2\pi), \quad \forall n \in \mathcal{N}, \quad (8)$$

which can be solved efficiently by reformulating it into a similar form as problem (6). As problem (8) is irrelevant to the AP's active beamforming, we can decompose the joint beamforming optimization into two sub-problems and solve them independently. Hence, we can avoid iterations between $\mathbf{w}$ and $\boldsymbol{\theta}$ and thus reduce the overall computational complexity.

B. Outer-loop Update of the Reflection Amplitude

Given the inner-loop beamforming solution $(\mathbf{w}, \boldsymbol{\theta})$, the next step is to update the outer-loop reflection amplitude ρ to further reduce the AP's transmit power. Note that the constraints (3b) and (3c) actually define the lower and upper bounds of the reflection amplitude ρ, respectively. Given the feasible region of ρ, we can further exploit the structural property of the optimal solution to problem (3), which will shed some insight on the algorithm design to search for the optimal reflection amplitude.

Proposition 1: *Given the beamforming solution* $(\boldsymbol{\theta}, \mathbf{w})$*, the upper bound on the reflection amplitude* $\rho_{\max}$ *for problem* (3) *is given as* $\rho_{\max} = \left(1 - \frac{N\mu}{\eta \|\mathbf{H}^H \mathbf{w}\|^2}\right)^{1/2}$*, while the lower bound* $\rho_{\min}$ *is the unique feasible solution to the quadratic equation* $a\rho^2 + b\rho + c = 0$*, where the constant coefficients* (a, b, c) *are given by* $a = |(\mathbf{H_f}\boldsymbol{\theta})^H \mathbf{w}|^2$*,* $b = 2\,\mathrm{Re}\left(\boldsymbol{\theta}^H \mathbf{H}_\mathbf{f}^H \mathbf{w}\mathbf{w}^H \mathbf{g}\right)$*, and* $c = |\mathbf{g}^H \mathbf{w}|^2 - \gamma_0$*, respectively.*

The proof for Proposition 1 is relegated to Appendix A. It is clear that Proposition 1 provides the feasible region for ρ, given the joint beamforming strategies $(\mathbf{w}, \boldsymbol{\theta})$. Considering the non-trivial case with non-empty feasible region for ρ, the following result further reveals the structural property of the optimal solution to problem (3), which will guide the search for the optimal reflection amplitude ρ in an iterative manner.

Proposition 2: *Assuming that problem* (3) *is feasible, the constraint in* (3c) *always holds with equality at optimum.*

The proof for this proposition is detailed in Appendix B. Proposition 2 implies an iterative search method for the optimal ρ. Specifically, given the feasible region $[\rho_{\min}, \rho_{\max}]$ determined by Proposition 1, we can update ρ in the next iteration as $\rho = (\rho_{\min} + \rho_{\max})/2$. This allows us to further update the beamforming strategies $(\mathbf{w}, \boldsymbol{\theta})$ by solving problems (6) and (7) iteratively in the AO framework. Such an iterative procedure terminates when the constraint (3c) holds with equality. The detailed solution procedure for problem (3) is shown in Algorithm 1. We set the termination condition as the objectives of two consecutive iterations fall within a predefined tolerance gap, ϵ. The convergence of Algorithm 1 is guaranteed by the following proposition.

Proposition 3: *Algorithm 1 always converges to a finite value.*

Proof: With a fixed ρ, it is clear that each iteration of the AO method for $(\mathbf{w}, \boldsymbol{\theta})$ will reduce the AP's transmit power. Besides, Proposition 2 reveals that the update to ρ can further reduce the AP's transmit power. As the objective in (3a) has a finite lower bound, this implies that the iterations in Algorithm 1 will eventually converge to a finite value. ■

C. An Illustrative Example of Algorithm 1

In this part, we provide an illustrative example to help understand the iterations in Algorithm 1. The feasibility of problem (3) is determined by the SNR and power budget constraints in (3b) and (3c), which define two lower bounds for the AP's transmit powers, denoted by $\|\mathbf{w}_1\|^2$ and $\|\mathbf{w}_2\|^2$, respectively. It is clear that $\|\mathbf{w}_1\|^2$ decreases with the increase of ρ while on the contrary $\|\mathbf{w}_2\|^2$ increases in ρ. In the following, we fix the IRS's phase vector $\boldsymbol{\theta}$ by solving problem (8) and then discuss the relations between ρ and $\mathbf{w}$.

1) Case I: Ideal IRS with neglectable power consumption: In this case, the optimization problem focuses on the receiver only and the AP's transmit beamforming can be simply aligned with the IRS-enhanced channel to the receiver. Given the receiver's SNR requirement γ_0, the AP's transmit power in the IRS-assisted system is limited by $\|\mathbf{w}_1\|^2_{\max} = \gamma_0/\|\mathbf{g}\|^2$, while the minimum transmit power is given by $\|\mathbf{w}_1\|^2_{\min} = \gamma_0/\|(\mathbf{g} + \mathbf{H_f}\boldsymbol{\theta})\|^2$ with $\rho = 1$. As shown in Fig. 2, the lower bound $\|\mathbf{w}_1\|^2$ is plotted as the dotted curve.

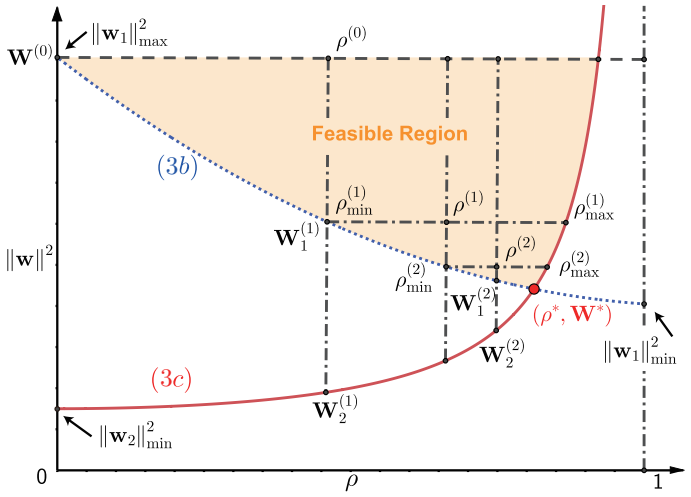

Fig. 2: An illustrative example of Algorithm 1.

2) Case II: Ideal receiver with neglectable SNR requirement: In this case, the optimization problem is only constrained by the IRS's power budget constraint. By setting $\rho = 0$ in the extreme case, the IRS can harvest the RF energy at the maximum rate, and thus the AP's minimum transmit power is given by (4). For different ρ, the lower bound is similarly evaluated by $\|\mathbf{w}_2\|^2 \triangleq \arg\min_{\mathbf{w}} \left\{\|\mathbf{w}\|^2 : \eta(1-\rho^2)\|\mathbf{H}^H\mathbf{w}\|^2 \geq N\mu\right\}$, which is plotted as the solid curve in Fig. 2.

The x-axis of Fig. 2 denotes different choices of the reflection amplitude ρ and y-axis represents the AP's transmit power. The shaded area in Fig. 2 denotes the feasible region of ρ and $\|\mathbf{w}\|^2$. The algorithm initializes with $\|\mathbf{w}^{(0)}\|^2$ and a small $\rho^{(0)}$. In each AO iteration, the AP's active beamforming $\mathbf{w}$ is firstly optimized by solving the SDP in (7), which falls in the feasible region in Fig. 2. After that, $\rho^{(1)}_{\min}$ and $\rho^{(1)}_{\max}$ can be evaluated in closed-form expressions by Proposition 2, and thus the reflection amplitude for the next iteration is updated as $\rho^{(1)} = (\rho^{(1)}_{\min} + \rho^{(1)}_{\max})/2$, as shown in Fig. 2. This procedure iterates until the difference $|\rho^{(k)}_{\max} - \rho^{(k)}_{\min}|$ or $|\|\mathbf{w}^{(k)}\|^2 - \|\mathbf{w}^{(k-1)}\|^2|$ falls in a predefined tolerance gap ϵ, as indicated in Algorithm 1.

IV. Robust Active and Passive Beamforming Optimization

In this part, we extend the power minimization problem (3) to a more practical case with inexact CSI. Due to the use of passive elements in IRS, the channel estimations involving the IRS are inevitably subject to estimation errors. The performance degradation due to channel uncertainty in an IRS-assisted system is seldom explored in an analytical way. In the sequel, we firstly propose a channel uncertainty model for the IRS-assisted channels, and then reformulate a robust counterpart of the power minimization problem (3). After that, we transform the robust counterpart to an efficiently tractable form that is appealing for our algorithm design.

We assume that the direct channel $\mathbf{g}$ from the AP to the receiver can be estimated accurately by the receiver in a

training process. In particular, the AP can send a known pilot information to the receiver with fixed transmit power. Meanwhile the IRS switches off its reflecting elements. The channel $\mathbf{g}$ can be recovered at the receiver based on the received signal samples. However, by using the passive scattering elements, the IRS faces the challenge of accurate channel estimation due to its inability for regular information exchange with the active RF transceivers. Without information decoding capability at the IRS, the channels $\mathbf{H}$ and $\mathbf{f}$ have to be estimated at either the AP or the receiver by overhearing the channel response.

A. Robust Counterpart and Reformulations

Due to the lack of channel samples, the channel $\mathbf{H}$ is typically subject to estimation errors, i.e., $\mathbf{H} = \bar{\mathbf{H}} + \mathbf{\Delta_h}$, where $\bar{\mathbf{H}}$ denotes the averaged channel matrix and $\mathbf{\Delta_h}$ denotes the error estimate of the channel matrix. We assume that the error estimate $\mathbf{\Delta_h}$ has limited power distribution, and thus we can define the uncertainty set $\mathbb{U}_\mathbf{h}$ for channel $\mathbf{H}$ as follows:

$$\mathbf{H} \in \mathbb{U}_\mathbf{h} \triangleq \{\mathbf{H} = \bar{\mathbf{H}} + \mathbf{\Delta_h} : \mathrm{Tr}(\mathbf{\Delta_h}^H \mathbf{\Delta_h}) \le \delta_\mathbf{h}^2\}, \quad (9)$$

where $\delta_\mathbf{h}$ denotes the power limits of error estimate $\mathbf{\Delta_h}$. A similar channel uncertainty model is also employed in [18], [20], [23]. The estimation of channel $\mathbf{f}$ becomes more difficult as the passive IRS generally cannot emit RF pilot signals for channel training. As such, the channel $\mathbf{f}$ has to be bundled with the channel $\mathbf{H}$ to form the cascaded channel $\mathbf{H_f}$, as defined in (2), which can be estimated at the receiver by overhearing the mixture of signals from the AP and the IRS's reflections. Similar to (9), we can define the uncertainty of the cascaded channel $\mathbf{H_f}$ as follows:

$$\mathbf{H_f} \in \mathbb{U}_\mathbf{f} \triangleq \{\mathbf{H_f} = \bar{\mathbf{H}}_\mathbf{f} + \mathbf{\Delta_f} : \mathrm{Tr}(\mathbf{\Delta_f}^H \mathbf{\Delta_f}) \le \delta_\mathbf{f}^2\}, \quad (10)$$

where $\delta_\mathbf{f}$ denotes the power limit of error estimate $\mathbf{\Delta_f}$ for the channel $\mathbf{H_f}$. The average estimate $\bar{\mathbf{H}}_\mathbf{f}$ and the power limit $\delta_\mathbf{f}$ are assumed to be known by historical measurements. Given the uncertainty models in (9) and (10), the robust counterpart of (3) can be formulated as follows:

$$\begin{aligned}
\min_{\mathbf{w},\theta,\rho} \quad & \|\mathbf{w}\|^2, && (11a)\\
\text{s.t.} \quad & \|(\mathbf{g} + \rho \mathbf{H_f}\theta)^H \mathbf{w}\|^2 \ge \gamma_0, \quad \forall\, \mathbf{H_f} \in \mathbb{U}_\mathbf{f}, && (11b)\\
& \eta(1-\rho^2)\|\mathbf{H}^H\mathbf{w}\|^2 \ge N\mu, \quad \forall\, \mathbf{H} \in \mathbb{U}_\mathbf{h}, && (11c)\\
& \rho \in [0,1] \text{ and } \theta_n \in [0, 2\pi) \quad \forall\, n \in \mathcal{N}. && (11d)
\end{aligned}$$

The constraints (11b) and (11c) define the receiver's worst-case SNR requirement and the IRS's worst-case power budget constraint, respectively. Now, we focus on the optimization of the IRS's reflection amplitude ρ and the joint beamforming strategies $(\mathbf{w}, \theta)$ in problem (11), which are closely coupled with the uncertain channels $\mathbf{H_f}$ and $\mathbf{H}$. In the sequel, we firstly explore equivalent reformulations to the constraints (11b)-(11c).

Proposition 4: *The constraint in* (11b) *bears the following equivalence:*

$$\rho^2 \mathbf{A} + \rho \mathbf{B} + \mathbf{C} \succeq 0, \quad (12)$$

where the coefficients $\mathbf{A}$, $\mathbf{B}$, *and* $\mathbf{C}$ *are given as follows:*

$$\begin{aligned}
\mathbf{A} &= \begin{bmatrix} \mathbf{\Theta} \otimes \mathbf{W} & (\mathbf{W}_c \bar{\mathbf{H}}_\mathbf{f})\mathrm{vec}(\mathbf{\Theta}) \\ \mathrm{vec}(\mathbf{\Theta})^H (\mathbf{W}_c \bar{\mathbf{H}}_\mathbf{f})^H & \mathrm{Tr}(\bar{\mathbf{H}}_\mathbf{f}^H \mathbf{W} \bar{\mathbf{H}}_\mathbf{f} \mathbf{\Theta}) \end{bmatrix},\\
\mathbf{B} &= \begin{bmatrix} \mathbf{0} & (\theta \otimes \mathbf{W})\mathbf{g} \\ \mathbf{g}^H(\theta \otimes \mathbf{W})^H & \mathbf{g}^H \mathbf{W} \bar{\mathbf{H}}_\mathbf{f} \theta + \theta^H \bar{\mathbf{H}}_\mathbf{f}^H \mathbf{W} \mathbf{g} \end{bmatrix},\\
\mathbf{C} &= \begin{bmatrix} t\mathbf{I}_{MN} & \mathbf{0} \\ \mathbf{0} & \mathbf{g}^H \mathbf{W} \mathbf{g} - \gamma_0 - t\delta_\mathbf{f}^2, \end{bmatrix},
\end{aligned}$$

for some $t \ge 0$, *where we define* $\mathbf{W}_c = \mathbf{I}_N \otimes \mathbf{W}$ *for notational convenience.* $\mathbf{W}$ *is a rank-one relaxation matrix of* $\mathbf{w}\mathbf{w}^H$. *Similarly,* $\mathbf{\Theta}$ *is the rank-one relaxation matrix of* $\theta\theta^H$.

The proof for Proposition 4 is relegated to Appendix C. It transforms the worst-case semi-infinite constraint in (11b) into a semidefinite matrix inequality. Given a fixed ρ, the matrix inequality in (12) is still in a non-convex form due to the bilinear coupling between $\mathbf{W}$ and $\mathbf{\Theta}$ (or θ). However, for any fixed $\mathbf{\Theta}$ or $\mathbf{W}$, constraint (12) becomes a linear matrix inequality with respect to the other decision variables. This implies that the AO method used for the non-robust problem in (3) can be applied similarly in optimizing $\mathbf{W}$ and $\mathbf{\Theta}$ in the robust case.

Proposition 5: *The constraint in* (11c) *bears the following equivalent reformulation.*

$$\begin{bmatrix} \mathbf{W}_c + \tau \mathbf{I}_{MN}, & \mathbf{W}_c \mathrm{vec}(\bar{\mathbf{H}}) \\ \mathrm{vec}(\bar{\mathbf{H}})^H \mathbf{W}_c, & \bar{\gamma} - \frac{N\mu}{\eta(1-\rho^2)} - \tau\delta_\mathbf{h}^2 \end{bmatrix} \succeq 0, \quad (13)$$

for some $\tau \ge 0$, *where we define* $\bar{\gamma} = \mathrm{vec}(\bar{\mathbf{H}})^H \mathbf{W}_c \mathrm{vec}(\bar{\mathbf{H}})$ *for notational convenience.*

The proof for Proposition 5 follows a similar idea to that for Proposition 4. The detailed proof is relegated to Appendix D. Note that the equivalence in (13) has a much simpler form, which is linear in $\mathbf{W}$ for some fixed ρ. Hence, we can reformulate the robust counterpart (11) as follows:

$$\min_{\rho, \mathbf{\Theta}_{n,n}=1, \mathbf{W} \succeq 0, t \ge 0, \tau \ge 0} \quad \{\mathrm{Tr}(\mathbf{W}) \,|\, (12) \text{ and } (13)\}. \quad (14)$$

Though problem (14) is still difficult to solve directly, we can consider a similar decomposition as that for the non-robust problem (3) and thus follow the two-stage optimization framework in Algorithm 1. In particular, we keep the search for ρ in the outer loop and then optimize $(\mathbf{W}, \mathbf{\Theta})$ in the inner loop with a fixed ρ. In the sequel, we present the details for each optimization stage.

B. Two-stage Robust Beamforming Optimization

1) Inner-loop beamforming optimization: Given a fixed reflection amplitude ρ in the outer loop, the inner-loop optimization of $(\mathbf{W}, \mathbf{\Theta})$ can follow a similar AO method as that in Algorithm 1. In particular, we can firstly initialize the phase vector θ and the corresponding phase matrix $\mathbf{\Theta}$ randomly. Hence, the matrix inequalities in (12) and (13) all become linear forms in terms of the active beamforming matrix $\mathbf{W}$ and the auxiliary variables (t, τ). On the other aspect, with fixed $\mathbf{W}$, the constraint in (12) also becomes a linear matrix inequality in terms of $\mathbf{\Theta}$. This implies that the inner-loop problem (14) with a fixed ρ can be easily handled by the

Algorithm 2 Two-stage Robust Beamforming Optimization with Channel Uncertainty

1: $\|\mathbf{w}_0\|^2 \leftarrow \infty$, $k \leftarrow 1$, $\epsilon \leftarrow 10^{-5}$, $\rho^{(0)} \leftarrow \epsilon_0$
2: Solve $\boldsymbol{\theta}$ according to (8) with $\bar{\mathbf{H}}_\mathbf{f}$
3: **while** $|\|\mathbf{w}_k\|^2 - \|\mathbf{w}_{k-1}\|^2| > \epsilon$
4: $k \leftarrow k+1$
5: **Update** $(\boldsymbol{\theta}, \mathbf{w})$:
Retrieve $(\boldsymbol{\theta}, \mathbf{w})$ in (8) and (16), respectively
Update $\mathbf{w}_k \leftarrow \mathbf{w}$
6: **Outer-loop update** ρ :
Retrieve $\rho_{\max}$ in (17a) by the bisection method
Retrieve $\rho_{\min}$ in (17b) by the bisection method
$\rho \leftarrow (\rho_{\min} + \rho_{\max})/2$
7: **end while**

AO method. Similar to the Max-Gain algorithm for the non-robust case, we can also simplify the inner-loop optimization by optimizing the IRS's phase vector $\boldsymbol{\theta}$ directly to enhance the equivalent channel $\|\mathbf{g} + \rho\mathbf{H}_\mathbf{f}\boldsymbol{\theta}\|^2$. Comparing to problem (8) for the non-robust case, the only difference for the robust case is that the channel matrix $\mathbf{H}_\mathbf{f}$ has to be replaced by its average estimate $\bar{\mathbf{H}}_\mathbf{f}$. Given the phase vector $\boldsymbol{\theta}$, the optimization of $\mathbf{w}$ can be also simplified into a convex problem:

Proposition 6: *Given the solution* $\boldsymbol{\theta}$ *to* (8)*, the constraint in* (12) *can be further simplified as:*

$$\begin{bmatrix} \rho^2\left(\boldsymbol{\theta}\boldsymbol{\theta}^H \otimes \mathbf{W}\right) + t\mathbf{I}_{MN} & \rho(\boldsymbol{\theta} \otimes \mathbf{W})\bar{\mathbf{g}} \\ \rho\bar{\mathbf{g}}^H(\boldsymbol{\theta} \otimes \mathbf{W})^H & \bar{\mathbf{g}}^H\mathbf{W}\bar{\mathbf{g}} - \gamma_0 - t\delta_\mathbf{f}^2 \end{bmatrix} \succeq 0, \tag{15}$$

which becomes a linear matrix inequality with the fixed ρ*.*

Proposition 6 is a direct result from Proposition 4. Note that the matrix coefficient $\boldsymbol{\theta}\boldsymbol{\theta}^H \otimes \mathbf{W}$ can be further simplified as $(\boldsymbol{\theta}\otimes\mathbf{W})(\boldsymbol{\theta}^H\otimes\mathbf{I}_M)$. The common term $\boldsymbol{\theta}\otimes\mathbf{W}$ in (15) is linear with regard to $\mathbf{W}$. As such, we can optimize $\mathbf{W}$ efficiently by solving the following SDP:

$$\min_{\mathbf{W}\succeq 0, t\geq 0, \tau \geq 0} \quad \{\mathrm{Tr}(\mathbf{W}) \,|\, (13) \text{ and } (15)\}. \tag{16}$$

The AP's beamforming vector $\mathbf{w}$ can be retrieved via eigenvalue decomposition if the solution $\mathbf{W}$ to problem (16) is rank-one, or approximated by GRM if $\mathbf{W}$ has a higher rank. By solving $\boldsymbol{\theta}$ and $\mathbf{w}$ independently in two sub-problems, the heuristic Max-Gain algorithm can avoid the iterations between $\mathbf{w}$ and $\boldsymbol{\theta}$, and thus improve the time efficiency compared to the AO method.

2) Outer-loop update of the reflection amplitude: The remaining task is to update the IRS's reflection amplitude ρ in the outer loop, based on the inner-loop solution $(\mathbf{w}, \boldsymbol{\theta})$ to problem (11). This can be performed following a similar idea for the non-robust case in Section III-B. Specifically, we firstly determine the upper and lower bounds on the reflection amplitude ρ and then update it to improve the objective in (11a). Given $(\mathbf{w}, \boldsymbol{\theta})$, the evaluation of $\rho_{\min}$ and $\rho_{\max}$ for the robust case depends on the feasibility check of two worst-case constraints in (11b) and (11c), respectively. As (11b) and (11c) have their SDR representations in (15) and (13), respectively. This can simplify the feasibility check by the following two sub-problems:

$$\rho_{\max} = \arg\max\{\rho \in (0,1) : \ (13) \text{ holds}\}, \tag{17a}$$
$$\rho_{\min} = \arg\min\{\rho \in (0,1) : \ (15) \text{ holds}\}. \tag{17b}$$

Though it is difficult to find closed-form expressions for $\rho_{\max}$ and $\rho_{\min}$, the following structural property implies that we can use a simple bisection method to search for them efficiently.

Proposition 7: *Given a feasible* ρ_o *to the matrix inequalities in* (13) *and* (15)*, we always have* ρ_1 *feasible to* (13) *for any* $\rho_1 \in (0, \rho_o)$ *and* ρ_2 *feasible to* (15) *for any* $\rho_2 \in (\rho_o, 1)$*.*

The proof of Proposition 7 is straightforward by an inspection of (12) and (13). Given the initialization $\rho_{\min} = 0$ and $\rho_{\max} = 1$, we firstly try $\rho = (\rho_{\min} + \rho_{\max})/2$ and check whether (13) is a positive semidefinite matrix. Then, we can tune down ρ if it is true or increase it if it is not true. This leads to the lower bound $\rho_{\min}$ at the convergence. The upper bound $\rho_{\max}$ can be determined by a similar procedure. The detailed solution procedure is given in Algorithm 2, which shares a similar flow of Algorithm 1. It is clear that Algorithm 2 follows an AO framework. Within each iteration, there are three steps to update $\mathbf{w}$, $\boldsymbol{\theta}$, and ρ, respectively. Each step relates to the solution of an SDP in the following standard form [39]: $\min_{\mathbf{x}\in\mathbb{R}^n}\left\{\mathbf{c}^T\mathbf{x} \mid A_i(\mathbf{x}) \succeq 0, \ \forall i = 1, \ldots, K\right\}$, which can be solved efficiently by the interior-point algorithm with the computational complexity given by $\mathcal{O}\left((\sum_i^K m_i)^{1/2}\left(n^2\sum_i^K m_i^2 + n\sum_i^K m_i^3\right)\right)$. Here m_i stands for the size of the matrix variable in each of the matrix inequalities $A_i(\mathbf{x}) \succeq 0$ and K is the number of matrix inequalities. Accordingly, we can evaluate the computational complexity in one iteration as that in (18). Note that the update of the reflection magnitude ρ depends on the evaluation of two extreme points, denoted as $\rho_{\min}$ and $\rho_{\max}$, respectively. Each point is determined by solving a set of SDPs via the bisection method with the error tolerance ε. Since the number of the IRS's reflecting elements are much larger than the number of the AP's antennas, i.e., $N \gg M$, the overall computational complexity is practically dominated by the term $M^{5.5}N^{3.5}$. As such, the overall computational complexity of the proposed algorithm can be characterized by $\mathcal{O}\left(\left(M^{5.5} + \log_2(\frac{1}{\varepsilon})M^{3.5}\right)N^{3.5}I_{\max}\right)$, where $I_{\max}$ denotes the maximum iterations of Algorithm 2.

V. Numerical Results

In this part, we verify the robust beamforming optimization algorithms and evaluate the performance variations with different system parameters, including channel uncertainty, the receiver's SNR requirement, the size of IRS, and the IRS's deployment location. The network topology in simulations is shown in Fig. 3. The AP locates at $(0, 0)$ and the IRS locates at $(d_{\text{AI}}, 0)$. The receiver locates at (d_0, d_v) and the distances from the AP to the IRS and from the IRS to the receiver are denoted by d_{AR} and d_{IR}, respectively. We set $d_v = 2$ m, $d_0 = 50$ m, and $d_{\text{AI}} = 5$ m in the simulations unless otherwise specified. We consider the AP with $M = 4$ antennas and the IRS with $20 \sim 180$ reflecting elements. Similar to [10], the path loss

$$\mathcal{O}\left(\underbrace{M^{6.5}N^{2.5}+M^{5.5}N^{3.5}}_{\text{optimize } \mathbf{w}}+\underbrace{N^{2.5}+N^{3.5}}_{\text{optimize } \boldsymbol{\theta}}+\underbrace{2\left(M^{2.5}N^{2.5}+M^{3.5}N^{3.5}\right)\log_2(1/\varepsilon)}_{\text{optimize } \rho}\right). \tag{18}$$

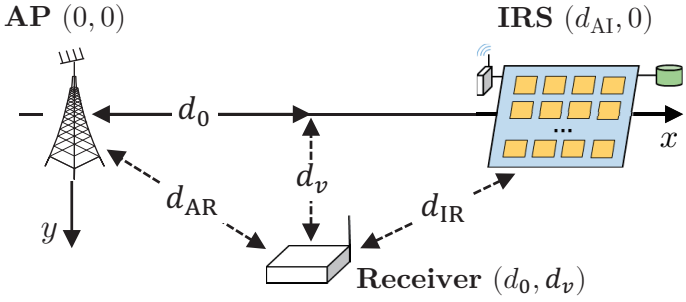

Fig. 3: Simulation environment of an IRS-assisted MISO system.

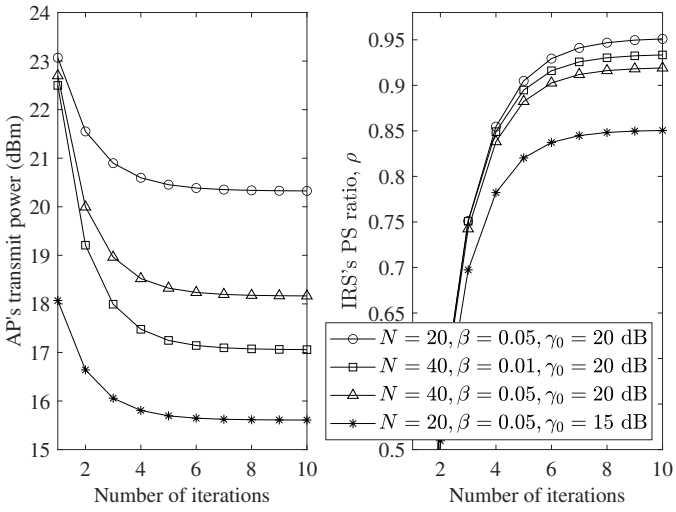

Fig. 4: The AP's transmit power and the IRS's reflection amplitude in Algorithm 2 with different channel uncertainties.

follows a log-distance propagation model. The loss exponents of the AP-IRS, AP-receiver and IRS-receiver channels are given by 2, 3.5, 2.8, respectively. The path loss at the reference distance (1 meter) is 30 dB. The energy consumption of one IRS element is set to 1 μW [40]. To characterize the channel uncertainties, we define *uncertainty levels* as $\beta_{\mathbf{h}} \triangleq \delta_{\mathbf{h}}^2/\text{Tr}(\bar{\mathbf{H}}\bar{\mathbf{H}}^H)$ and $\beta_{\mathbf{f}} \triangleq \delta_{\mathbf{f}}^2/\text{Tr}(\bar{\mathbf{H}}_{\mathbf{f}}\bar{\mathbf{H}}_{\mathbf{f}}^H)$, respectively, for the uncertain channels $\mathbf{H}$ and $\mathbf{H}_{\mathbf{f}}$. For simplicity, we consider $\beta = \beta_{\mathbf{h}} = \beta_{\mathbf{f}}$ in the following simulations. A larger β implies a higher variation of the channel conditions and thus larger errors in channel estimation. For each simulation setting, we run the experiment 10 times with randomly generated channel conditions and record the averaged performance.

A. Convergence of the Two-stage Optimization Algorithm

We firstly verify the convergence of the proposed algorithm and explain its efficacy. In Fig. 4, we show the convergence of the AP's transmit power and the IRS's reflection amplitude in Algorithm 2. Four groups of different parameter settings are evaluated. For each setting, the AP's transmit power starts with a relatively high value to ensure the fulfillment of the worst-case SNR requirement at the receiver and the worst-case power budget constraint at the IRS. As the algorithm iterates, the AP's transmit power decreases significantly within a few iterations and then converges to a small value meanwhile the reflection amplitude ρ increases to reflect more RF power to the receiver. By dynamically adjusting the operating parameters at both the AP and the IRS in an iterative manner, the AP can tune down its transmit power gradually while still maintaining the desired service provisioning to the receiver. For four groups of simulation settings, the algorithm is shown to converge within a few iterations as shown in Fig. 4, which verifies the efficacy of Algorithm 2. Besides, we observe that a small uncertainty factor β or a low SNR requirement γ_0 can lead to a reduced transmit power at the AP and also a lower reflection amplitude at the IRS. For example, for $(N,\beta) = (20, 0.05)$, the AP's transmit power is 15.61 dBm when the SNR requirement is set to 15 dB, the AP's transmit power increases to 20.32 dBm when the receiver increases its SNR requirement to 20 dB. Note that the 4.7 dB increase to the AP's transmit power is less than the 5 dB increase to the receiver's SNR requirement. This is due to the IRS's reconfigurability. When the AP's transmit power increases, the IRS can tune up its reflection amplitude and optimize its phase shifting matrix to reflect and focus more RF power towards the receiver.

B. The Price of Robustness

The price of robustness can be viewed as the increase of the AP's transmit power to maintain the same quality provisioning to the receiver under uncertain channel conditions. In Fig. 5(a), we compare the performance of the robust Algorithm 2 with that of Algorithm 1 for the non-robust case. We also show the baseline performances for non-IRS-assisted case and the IRS's random phase shifting scheme. Once we obtain the matrix solution $(\mathbf{W}, \boldsymbol{\Theta})$ within each iteration, we can apply the Gaussian randomization method (GRM) to derive the approximate rank-one solution $(\mathbf{w}, \boldsymbol{\theta})$. Our results in Fig. 5 shows that Algorithm 2, by using the GRM method, can achieve the same performance as that of Algorithm 2 without using the GRM method. This verifies the efficacy of Algorithm 2 in robust beamforming optimization.

Comparing Algorithm 2 with Algorithm 1, we observe a significant increase in the AP's transmit power. The increase becomes even higher with a larger uncertainty level. This is intuitive as the AP has to raise its transmit power when the channel becomes highly fluctuating to met the receiver's SNR requirement or the IRS's power budget constraint. Such an

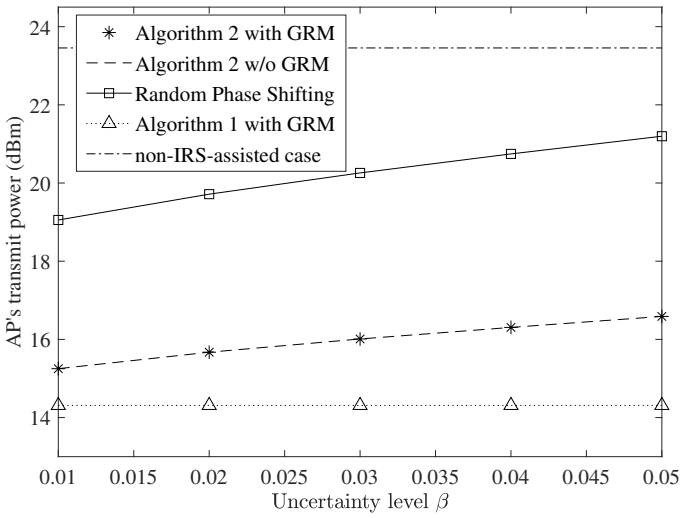

(a) AP's increasing power as the price of robustness.

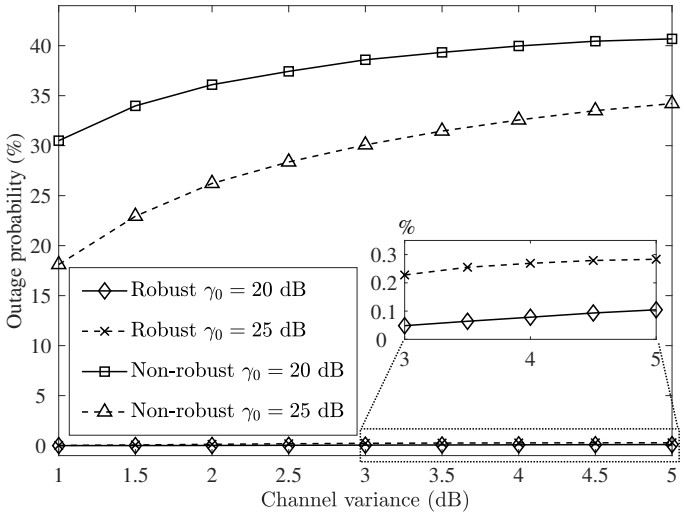

(b) Robustness ensures the reduced outage probabilities.

Fig. 5: Performance comparison between the robust and the non-robust algorithms.

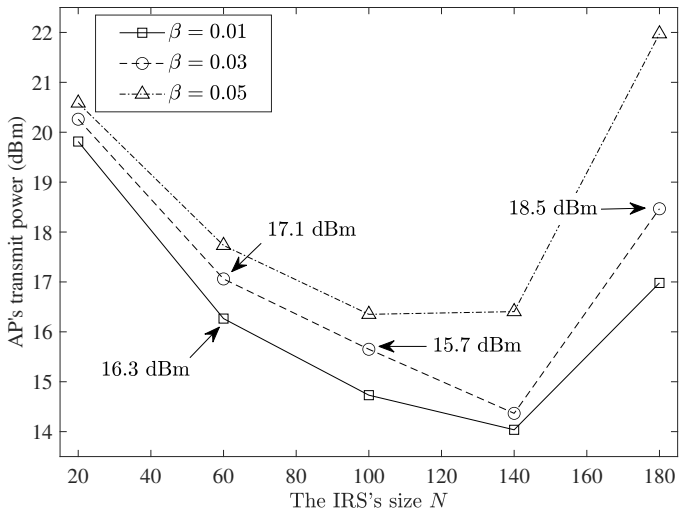

Fig. 6: A larger-size IRS can be used to fight against channel uncertainties.

increase in the AP's transmit power represents the price of robustness to fight against the channel uncertainties. For example, when $\beta = 0.01$, the AP's transmit power in Algorithm 2 is increased by 24% comparing to that in Algorithm 1. Such an increase comes up to 67% when $\beta = 0.05$. However, we also observe that the robust beamforming design in Algorithm 2 achieves significant power saving comparing to the non-IRS-assisted case or the random phase shifting scheme. In particular, when $\beta = 0.05$, the AP' transmit power can be saved by about 60% comparing to random phase shifting scheme and about 80% comparing to the non-IRS-assisted case.

An outage event occurs when either the receiver's SNR requirement is not fulfilled or the IRS's power budget constraint becomes failed due to the channel uncertainties. For a comparison, we also evaluate the outage performance of the non-robust Algorithm 1. In the simulation, the channels are generated randomly with the variance ranging from 1 to 5 dB. Both the robust and the non-robust algorithms estimate the CSI with the channel observations. The non-robust Algorithm 1 is implemented with the averaged channel estimations, while the robust Algorithm 2 allows the channel conditions to be fluctuating within a predefined range, which is characterized by the uncertainty level β. This provides extra protection for the receiver's SNR and the IRS's power budget constraints. In Fig. 5(b), we show the outage probabilities against different channel variances. We observe that barely no outage happens in the robust Algorithm 2. The outage probability of the non-robust Algorithm 1 is significantly larger than that of the robust case, and is further increasing with the channels' variance of fluctuation. Besides, the outage performance of the non-robust Algorithm 1 is very sensitive to the increase of the receiver's SNR requirement.

C. IRS's Size and Uncertainty Tradeoffs

We then evaluate the impact of IRS's size on the AP's minimum transmit power by varying N from 20 to 180. The receiver's SNR requirement is fixed at 20 dBm. It is obvious on one hand that a higher uncertainty level always implies a higher transmit power at the AP for a fixed size of the IRS. On the other hand, by increasing the IRS's size, it becomes possible to compensate for the performance loss due to the channel uncertainty. As shown in Fig. 6, given the IRS's size $N = 60$, the minimum required transmit power at the AP will be increased from 16.3 dBm to 17.3 dBm if the uncertainty level increases from $\beta = 0.01$ to $\beta = 0.03$. However, instead of increasing the AP's transmit power, we can also increase the IRS's size from $N = 60$ to $N = 100$ to fight against the channel uncertainty. As such, the AP's minimum transmit power for $\beta = 0.03$ can be reduced to 15.7 dBm, which is even less than that of the case with $(N = 60, \beta = 0.01)$. The reason is that a larger-size IRS can provide more channel gain in the AP-IRS-receiver link and thus improve the receiver's SNR and also reduce the AP's transmit power.

However, such a benefit diminishes when the IRS's size exceeds a certain value due to the IRS's power budget constraint.

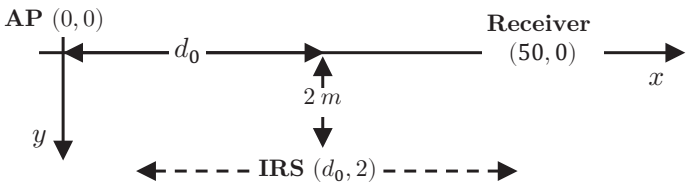

Fig. 7: Simulation topology to evaluate the IRS's deployment.

For example, the minimum transmit power required by the AP is raised up to 18.5 dBm with 180 elements under $\beta = 0.03$, which is about 2.8 dB higher than that with 100 elements. The reason is that the energy consumption of the IRS increases with its size linearly. However, the energy harvesting of the IRS does not increase linearly with its size since the AP's beamforming cannot targets at every single element on the IRS at the same time. In summary, increasing the IRS's size provides an efficient way for power saving at the AP. However, the large-size IRS also requires more energy harvesting from the AP, which implies that we need to carefully design the IRS's size to balance between its power demand and the performance gain under uncertain channel conditions.

D. Deploying IRS Closer to the AP

Given the IRS's power budget constraint, the IRS's deployment location is also an important design aspect to minimize the AP's transmit power subject to the receiver's SNR requirement. Note that the IRS is self-powered by harvesting RF energy from the AP's beamforming signals. Hence, we expect that it is preferable to deploy IRS closer to the AP. To verify this result, we consider the simulation topology in Fig. 7, where the AP and the receiver locate at $(0,0)$ and $(50,0)$, respectively. The IRS locates at $(d_0,2)$, where d_0 denotes the horizontal distance between the AP and the IRS. The IRS's size is fixed at $N = 60$ and the receiver's SNR requirement is set to 20 dB. When the IRS moves far away from the AP, we observe that the AP's transmit power also increases as shown in Fig. 8(a), while the IRS's reflection amplitude decreases as shown in Fig. 8(b). The reason lies in two folds. Firstly, the AP-IRS channel becomes worse off as the IRS moves away from the AP, which implies a reduced energy harvesting rate at the IRS. As such, the AP has to increase its transmit power and the IRS has to tune down its reflection amplitude to sustain the IRS's operations. Secondly, the product of the AP-IRS and the IRS-receiver channels deteriorates as the IRS locates in the middle of the AP and the receiver, similar to the observations in [10]. This requires a higher transmit power at the AP to maintain the same quality provisioning to the receiver. In the extreme case, when the IRS is deployed far away from the AP, the IRS may be no longer self-sustainable by harvesting energy from the AP's beamforming signals, given the energy consumption of scattering elements. In this case, the MISO downlink system tends to operate independently without the IRS's assistance. For example, given $\mu = 5$ μW, the IRS-assisted system performs no better than the non-IRS-assisted system when the horizontal distance between the IRS and the AP is larger than 15 m.

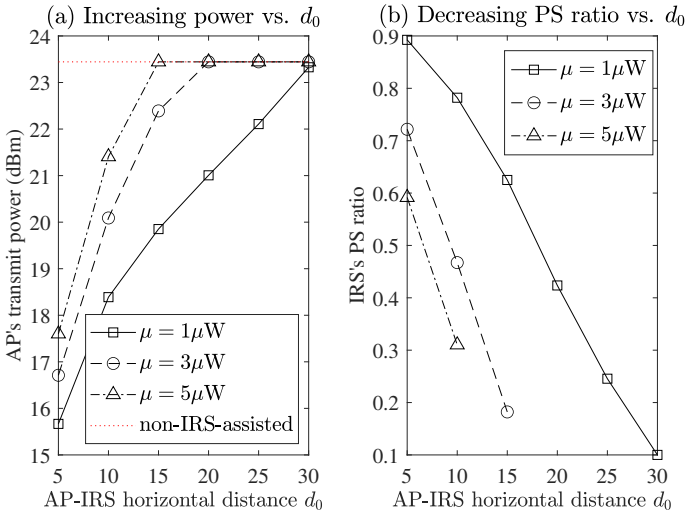

Fig. 8: The AP's transmit power and the IRS's reflection amplitude change with the IRS's deploying locations.

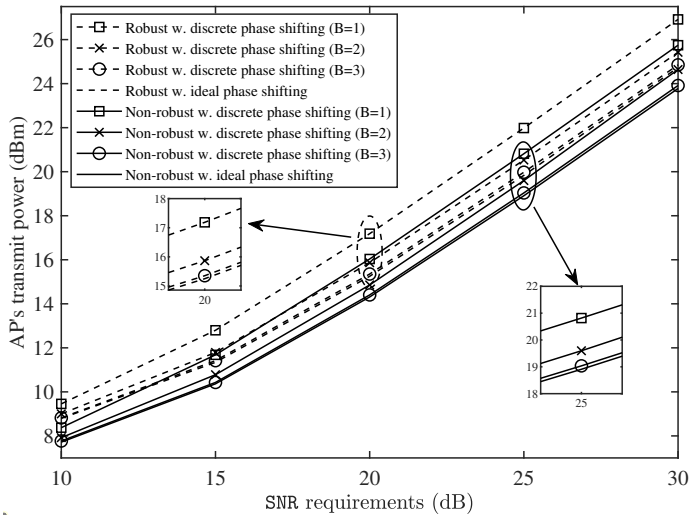

Fig. 9: Performance evaluation of discrete phase shifting for both robust and non-robust cases.

E. Higher Transmit Power under Discrete Phase Shifting

Finally, we consider a more practical scenario with discrete phase shifting at the IRS. In this case, the IRS's phase shifting is given by $\theta_n = e^{j\alpha_n}$, where α_n is chosen from a discrete set $\left\{0, \frac{2\pi}{L}, \ldots, \frac{2\pi(L-1)}{L}\right\}$, where $L = 2^B$ is the total number of phase shifting levels and B denotes the number of bits used to encode different phase shifts. Once we find the optimal continuous phase shifting scheme, denoted by $\theta_n^* = e^{j\alpha_n^*}$, we can always find the corresponding discrete phase shifting by projection: $l^* = \arg\min_{l\in[1,L]} |\theta_n^* - e^{j\alpha_{n,l}}|$, for each $n \in \mathcal{N}$, where $\alpha_{n,l} = 2\pi(l-1)/L$ and $l \in \{1,\ldots,L\}$. We set $(M,N) = (4,60)$ and vary the receiver's SNR requirement from 10 dB to 30 dB. The AP's optimal transmit power under both robust and non-robust cases are evaluated and shown in Fig. 9. The IRS's discrete phase shifting scheme is also evaluated as a benchmark. As shown in Fig. 9, for both robust and non-robust cases, the discrete phase shifting scheme

requires a higher transmit power at the AP compared to that of the ideal continuous phase shifting scheme. Fortunately, the IRS with discrete phase shifting can still provide significant performance gain. For $B = 3$, the discrete phase shifting achieves nearly the same performance as that of the ideal continuous phase shifting scheme.

VI. Conclusions

In this paper, we have considered an IRS-assisted multiple-input single-output wireless downlink system, in which the IRS works in a self-sustainable manner by harvesting energy from the radio frequency transmitter in the power splitting protocol. We have proposed the joint active and passive beamforming problem as well as its robust counterpart against channel uncertainties. By exploiting the problem structure, a two-stage optimization framework has been devised to solve both design problems in the non-robust and robust cases. Extensive numerical results have revealed that our proposed algorithm is efficacy to balance the IRS's energy budget and the receiver's signal enhancement by tuning IRS's reflection amplitude, even with uncertain channel conditions. Besides, a more practical discrete phase shifting scheme with 3-bit phase resolution can achieve nearly the same performance as that of the continuous phase shifting scheme.

Appendix

A. Proof for Proposition 1

Proof: The upper bound of ρ, denoted by $\rho_{\max}$, can be easily determined by solving the equation in the constraint (3c), resulting in $\rho_{\max} = \left(1 - \frac{N\mu}{\eta\|\mathbf{H}^H\mathbf{w}\|^2}\right)^{1/2}$. Similarly, the lower bound of ρ, denoted by $\rho_{\min}$, is determined by solving the equation in constraint (3b), which can be expanded as follows:

$$\rho^2|(\mathbf{H_f}\boldsymbol{\theta})^H\mathbf{w}|^2 + \rho\left(2\,\mathrm{Re}\left(\boldsymbol{\theta}^H\mathbf{H_f}^H\mathbf{w}\mathbf{w}^H\right)\mathbf{g}\right) + |\mathbf{g}^H\mathbf{w}|^2 - \gamma_0 = 0. \tag{19}$$

Note that (19) is a quadratic equation in the form of $a\rho^2 + b\rho + c = 0$ with the constant coefficients given by $a = |(\mathbf{H_f}\boldsymbol{\theta})^H\mathbf{w}|^2$, $b = 2\,\mathrm{Re}\left(\boldsymbol{\theta}^H\mathbf{H_f}^H\mathbf{w}\mathbf{w}^H\right)\mathbf{g}$, and $c = |\mathbf{g}^H\mathbf{w}|^2 - \gamma_0$, respectively. Non-trivially, it can be verified that $a > 0$, $b > 0$, $c < 0$, and $a + b + c \geq 0$. The reason is that a denotes the received signal strength via the AP-IRS-receiver link. Besides, b denotes the real part of inner product of the IRS-assisted signal and the direct beamforming signal. Hence, we can expect that $b > 0$ as the IRS-assisted link is an enhancement of the direct link. Furthermore, to motivate the use of IRS, we can expect that $c < 0$, which means that the received signal strength via the direct link is unable to meet the receiver's SNR requirement. Lastly, by setting $\rho = 1$ in (3b) and (19), we expect that $a + b + c > 0$, implying that the receiver's SNR requirement can be satisfied in the ideal case with zero energy consumption at the IRS. With these properties, we can solve the lower bound of ρ as the unique solution to the quadratic equation in (19), which is given by $\rho_{\min} = (\sqrt{b^2 - 4ac} - b)/2a \in (0, 1)$. ■

B. Proof for Proposition 2

Proof: We prove this proposition by using contradiction theory. We assume that $(\rho, \mathbf{w})$ is optimal to problem (3) and the constraint (3c) holds with strict inequality. Depending on the constraint (3b), we will have different strategies as follows: 1) If (3b) holds with strict inequality, it is clear that we can properly scale down $\mathbf{w}$ by a scalar factor $s < 1$ such that both constraints in (3b) and (3c) still hold. The scaling $s\mathbf{w}$ apparently leads to a better objective in (3a), which brings a contradictory to our assumption. 2) If (3b) holds with equality, we can still construct a new solution that leads to a reduced transmit power. In this case, the inequality (3b) always holds when we increase ρ. Let $\rho_{\min}$ and $\rho_{\max}$ denote the lower and upper bounds of ρ with the fixed $\mathbf{w}$, respectively. We then have the following equations:

$$|(\mathbf{g} + \rho_{\min}\mathbf{H_f}\boldsymbol{\theta})^H\mathbf{w}|^2 = \gamma_0, \tag{20a}$$

$$\eta(1 - \rho_{\max}^2)\|\mathbf{H}^H\mathbf{w}\|^2 = N\mu. \tag{20b}$$

Therefore, we can simple set $\rho_m = (\rho_{\min} + \rho_{\max})/2$ that ensures strict inequalities in both (3b) and (3c). This becomes exactly the first case, in which we can scale down $\mathbf{w}$ and achieve a reduced transmit power. Specifically, the scaling factor can be set as follows:

$$s = \min\left\{\frac{\gamma_0}{|(\mathbf{g} + \rho_m\mathbf{H_f}\boldsymbol{\theta})^H\mathbf{w}|^2}, \frac{N\mu}{(1 - \rho_m^2)\|\mathbf{H}^H\mathbf{w}\|^2}\right\}.$$

It is obvious that for any case above we can always improve the objective function, which verifies that the constraint in (3c) has to hold with equality at optimum. ■

C. Proof for Proposition 4

Proof: Considering the uncertainty of channel matrix $\mathbf{H_f} = \bar{\mathbf{H}}_\mathbf{f} + \boldsymbol{\Delta}_\mathbf{f}$, we can define $\bar{\mathbf{g}} = \mathbf{g} + \rho\bar{\mathbf{H}}_\mathbf{f}\boldsymbol{\theta}$ for notational convenience and rewrite (11b) as follows:

$$|\bar{\mathbf{g}}^H\mathbf{w} + \rho\,(\boldsymbol{\Delta}_\mathbf{f}\boldsymbol{\theta})^H\mathbf{w}|^2 \geq \gamma_0, \forall\ \mathbf{H_f} \in \mathbb{U}_\mathbf{f}. \tag{21}$$

Let $\mathbf{d_f} = \boldsymbol{\Delta}_\mathbf{f}\boldsymbol{\theta}$ for notational convenience and define semidefinite matrix such that $\mathbf{W} \succeq \mathbf{w}\mathbf{w}^H$. The LHS of (11b) can be easily transformed as follows:

$$\begin{aligned}&|\bar{\mathbf{g}}^H\mathbf{w} + \rho\mathbf{d_f}^H\mathbf{w}|^2\\ &= \rho^2\mathbf{d_f}^H\mathbf{W}\mathbf{d_f} + \bar{\mathbf{g}}^H\mathbf{W}\bar{\mathbf{g}} + \rho\bar{\mathbf{g}}^H\mathbf{W}\mathbf{d_f} + \rho\mathbf{d_f}^H\mathbf{W}\bar{\mathbf{g}}\\ &= \rho^2\mathrm{Tr}\left(\boldsymbol{\Delta}_\mathbf{f}^H\mathbf{W}\boldsymbol{\Delta}_\mathbf{f}\boldsymbol{\theta}\boldsymbol{\theta}^H\right) + \bar{\mathbf{g}}^H\mathbf{W}\bar{\mathbf{g}}\\ &\quad + \rho\mathrm{Tr}\left(\boldsymbol{\Delta}_\mathbf{f}^H\mathbf{W}\bar{\mathbf{g}}\boldsymbol{\theta}^H\right) + \rho\mathrm{Tr}\left(\boldsymbol{\theta}\bar{\mathbf{g}}^H\mathbf{W}\boldsymbol{\Delta}_\mathbf{f}\right).\end{aligned} \tag{22}$$

In the sequel, we have $\mathrm{Tr}(\mathbf{A}^H\mathbf{B}) = \mathrm{vec}(\mathbf{A})^H\mathrm{vec}(\mathbf{B})$ and $\mathrm{vec}(\mathbf{ABC}) = (\mathbf{C}^H \otimes \mathbf{A})\mathrm{vec}(\mathbf{B})$. As such, we can further rewrite (22) as follows:

$$\begin{aligned}&|\bar{\mathbf{g}}^H\mathbf{w} + \rho\mathbf{d_f}^H\mathbf{w}|^2\\ &= \rho^2\mathrm{vec}(\boldsymbol{\Delta}_\mathbf{f})^H(\boldsymbol{\theta}\boldsymbol{\theta}^H \otimes \mathbf{W})\mathrm{vec}(\boldsymbol{\Delta}_\mathbf{f}) + \bar{\mathbf{g}}^H\mathbf{W}\bar{\mathbf{g}}\\ &\quad + \rho\bar{\mathbf{g}}^H(\boldsymbol{\theta} \otimes \mathbf{W})^H\mathrm{vec}(\boldsymbol{\Delta}_\mathbf{f}) + \rho\mathrm{vec}(\boldsymbol{\Delta}_\mathbf{f})^H(\boldsymbol{\theta} \otimes \mathbf{W})\bar{\mathbf{g}}.\end{aligned} \tag{23}$$

Till now, the LHS of (21) can be rewritten in a quadratic form, i.e., $\mathbf{x}^H\mathbf{M}\mathbf{x} \geq 0$, where $\mathbf{x} = \begin{bmatrix}\mathrm{vec}(\boldsymbol{\Delta}_\mathbf{f})\\ 1\end{bmatrix}$ and the matrix

coefficient $\mathbf{M}$ is given as follows:

$$\mathbf{M} = \begin{bmatrix} \rho^2 \left(\boldsymbol{\theta}\boldsymbol{\theta}^H \otimes \mathbf{W} \right) & \rho(\boldsymbol{\theta} \otimes \mathbf{W})\bar{\mathbf{g}} \\ \rho\bar{\mathbf{g}}^H(\boldsymbol{\theta} \otimes \mathbf{W})^H & \bar{\mathbf{g}}^H\mathbf{W}\bar{\mathbf{g}} - \gamma_0 \end{bmatrix}.$$

It is easy to see from (21) that $\mathbf{x}^H\mathbf{M}\mathbf{x} \geq 0$ holds for any $\boldsymbol{\Delta}_\mathbf{f}$ satisfying $\mathrm{vec}(\boldsymbol{\Delta}_\mathbf{f})^H\mathrm{vec}(\boldsymbol{\Delta}_\mathbf{f}) \leq \delta_\mathbf{f}^2$. By S-Lemma [41], we can always find some $t \geq 0$ such that

$$\begin{bmatrix} \rho^2 \left(\boldsymbol{\theta}\boldsymbol{\theta}^H \otimes \mathbf{W} \right) + t\mathbf{I}_{MN} & \rho(\boldsymbol{\theta} \otimes \mathbf{W})\bar{\mathbf{g}} \\ \rho\bar{\mathbf{g}}^H(\boldsymbol{\theta} \otimes \mathbf{W})^H & \bar{\mathbf{g}}^H\mathbf{W}\bar{\mathbf{g}} - \gamma_0 - t\delta_\mathbf{f}^2 \end{bmatrix} \succeq 0. \tag{24}$$

Note that the IRS-assisted channel $\bar{\mathbf{g}} = \mathbf{g} + \rho\bar{\mathbf{H}}_\mathbf{f}\boldsymbol{\theta}$ also depends on the choice of phase shift vector $\boldsymbol{\theta}$. In the sequel, we rearrange matrix terms in (24) and verify that the matrix inequality is linear in terms of $\boldsymbol{\theta}$ and its semidefinite relaxation $\boldsymbol{\Theta} \succeq \boldsymbol{\theta}\boldsymbol{\theta}^H$. It is clear that $\bar{\mathbf{g}}^H\mathbf{W}\bar{\mathbf{g}}$ can be rewritten as follows:

$$\begin{aligned} \bar{\mathbf{g}}^H\mathbf{W}\bar{\mathbf{g}} \;=\; & \rho\mathbf{g}^H\mathbf{W}\bar{\mathbf{H}}_\mathbf{f}\boldsymbol{\theta} + \rho\boldsymbol{\theta}^H\bar{\mathbf{H}}_\mathbf{f}^H\mathbf{W}\mathbf{g} \\ & + \mathbf{g}^H\mathbf{W}\mathbf{g} + \rho^2\mathrm{Tr}(\bar{\mathbf{H}}_\mathbf{f}^H\mathbf{W}\bar{\mathbf{H}}_\mathbf{f}\boldsymbol{\Theta}), \end{aligned} \tag{25}$$

which is linear with respect to $\boldsymbol{\theta}$ and $\boldsymbol{\Theta}$ for any fixed $(\rho, \mathbf{W})$. Furthermore, the off-diagonal element in (24) can be expanded as $\rho(\boldsymbol{\theta} \otimes \mathbf{W})\bar{\mathbf{g}} = \rho(\boldsymbol{\theta} \otimes \mathbf{W})\mathbf{g} + \rho^2(\boldsymbol{\theta} \otimes \mathbf{W})\bar{\mathbf{H}}_\mathbf{f}\boldsymbol{\theta}$, where the second term can be further transformed by using the following equalities:

$$(\boldsymbol{\theta} \otimes \mathbf{W})\bar{\mathbf{H}}_\mathbf{f}\boldsymbol{\theta} = (\mathbf{W}_c\bar{\mathbf{H}}_\mathbf{f})(\boldsymbol{\theta} \otimes \boldsymbol{\theta}) = (\mathbf{W}_c\bar{\mathbf{H}}_\mathbf{f})\mathrm{vec}(\boldsymbol{\Theta}), \tag{26}$$

where $\mathbf{W}_c = \mathbf{I}_N \otimes \mathbf{W}$ for notational convenience. By substituting (25) and (26) into (24), we can arrive at the equivalent semidefinite representation in (12). ■

D. Proof for Proposition 5

Proof: The proof of Proposition 5 follows a similar idea to that for Proposition 4 by rewriting the semi-infinite constraint (11c) into a quadratic form. Let $\gamma_0 = \|\mathbf{H}^H\mathbf{w}\|^2$ and $\bar{\gamma}_0 = \|\bar{\mathbf{H}}^H\mathbf{w}\|^2$. We have the following reformulations:

$$\begin{aligned} \gamma_0 &= \mathbf{w}^H\left(\bar{\mathbf{H}} + \boldsymbol{\Delta}_\mathbf{h}\right)\left(\bar{\mathbf{H}} + \boldsymbol{\Delta}_\mathbf{h}\right)^H\mathbf{w} \\ &= \mathbf{w}^H\boldsymbol{\Delta}_\mathbf{h}\boldsymbol{\Delta}_\mathbf{h}^H\mathbf{w} + \mathbf{w}^H\boldsymbol{\Delta}_\mathbf{h}\bar{\mathbf{H}}^H\mathbf{w} + \mathbf{w}^H\bar{\mathbf{H}}\boldsymbol{\Delta}_\mathbf{h}^H\mathbf{w} + \bar{\gamma}_0 \\ &= \mathrm{Tr}(\boldsymbol{\Delta}_\mathbf{h}^H\mathbf{W}\boldsymbol{\Delta}_\mathbf{h}) + \mathrm{Tr}(\boldsymbol{\Delta}_h^H\mathbf{W}\bar{\mathbf{H}}) + \mathrm{Tr}(\bar{\mathbf{H}}^H\mathbf{W}\boldsymbol{\Delta}_\mathbf{h}) + \bar{\gamma}_0. \end{aligned}$$

Similarly, by using the trace equalities, i.e., $\mathrm{Tr}(\mathbf{A}^H\mathbf{B}) = \mathrm{vec}(\mathbf{A})^H\mathrm{vec}(\mathbf{B})$ and $\mathrm{vec}(\mathbf{AB}) = (\mathbf{I}_N \otimes \mathbf{A})\,\mathbf{B}$ for the matrices $\mathbf{A}$ and $\mathbf{B}$ with the dimensions $M \times M$ and $M \times N$, respectively, we can rewrite γ_0 as follows:

$$\begin{aligned} \gamma_0 = \mathrm{vec}(\boldsymbol{\Delta}_\mathbf{h})^H\mathbf{W}_c\mathrm{vec}(\boldsymbol{\Delta}_\mathbf{h}) + \mathrm{vec}(\boldsymbol{\Delta}_\mathbf{h})^H\mathbf{W}_c\mathrm{vec}(\bar{\mathbf{H}}) \\ + \mathrm{vec}(\bar{\mathbf{H}})^H\mathbf{W}_c\mathrm{vec}(\boldsymbol{\Delta}_\mathbf{h}) + \bar{\gamma}_0, \end{aligned} \tag{27}$$

where $\mathbf{W}_c = \mathbf{I}_N \otimes \mathbf{W}$. Note that we can write $\bar{\gamma}_0$ as $\bar{\gamma}_0 = \mathbf{vec}(\bar{\mathbf{H}})^H\mathbf{W}_c\mathrm{vec}(\bar{\mathbf{H}})$. As such, we can reformulate the constraint (11c) into a quadratic form of the uncertain vector $\mathrm{vec}(\boldsymbol{\Delta}_\mathbf{h})$. Note that $\mathrm{vec}(\boldsymbol{\Delta}_\mathbf{h})^H\mathrm{vec}(\boldsymbol{\Delta}_\mathbf{h}) = \mathrm{Tr}(\boldsymbol{\Delta}_\mathbf{h}^H\boldsymbol{\Delta}_\mathbf{h}) \leq \delta_\mathbf{h}^2$. By S-Lemma, the worst-case power budget constraint in (11c) can be equivalently represented by (13). ■

REFERENCES

[1] M. D. Renzo, M. Debbah, D. T. P. Huy, A. Zappone, M. Alouini, C. Yuen, V. Sciancalepore, G. C. Alexandropoulos, J. Hoydis, H. Gacanin, J. de Rosny, A. Bounceu, G. Lerosey, and M. Fink, "Smart radio environments empowered by AI reconfigurable meta-surfaces: An idea whose time has come," *EURASIP J. Wirel. Commun. Netw.*, vol. 129, no. 1, pp. 1–20, May 2019.

[2] S. Gong, X. Lu, D. T. Hoang, D. Niyato, L. Shu, D. I. Kim, and Y.-C. Liang, "Toward smart wireless communications via intelligent reflecting surfaces: A contemporary survey," *IEEE Commun. Surv. Tut.*, vol. 22, no. 4, pp. 2283–2314, Fourthquarter 2020.

[3] C. Liaskos, A. Tsioliaridou, A. Pitsillides, S. Ioannidis, and I. Akyildiz, "Using any surface to realize a new paradigm for wireless communications," *Commun. ACM*, vol. 61, no. 11, pp. 30–33, Oct. 2018.

[4] Q. Wu, S. Zhang, B. Zheng, C. You, and R. Zhang, "Intelligent reflecting surface-aided wireless communications: A tutorial," *IEEE Trans. Commun.*, vol. 69, no. 5, pp. 3313–3351, May 2021.

[5] Q. Wu and R. Zhang, "Towards smart and reconfigurable environment: Intelligent reflecting surface aided wireless network," *IEEE Commun. Mag.*, vol. 58, no. 1, pp. 106–112, Jan. 2020.

[6] Z. Chu, P. Xiao, M. Shojafar, D. Mi, J. Mao, and W. Hao, "Intelligent reflecting surface assisted mobile edge computing for internet of things," *IEEE Wireless Commun. Lett.*, vol. 10, no. 3, pp. 619–623, Mar. 2021.

[7] T. Bai, C. Pan, H. Ren, Y. Deng, M. Elkashlan, and A. Nallanathan, "Resource allocation for intelligent reflecting surface aided wireless powered mobile edge computing in OFDM systems," *IEEE Trans. Wireless Commun.*, vol. 20, no. 8, pp. 5389–5407, Aug. 2021.

[8] Z. Chu, Z. Zhu, F. Zhou, M. Zhang, and N. Al-Dhahir, "Intelligent reflecting surface assisted wireless powered sensor networks for internet of things," *IEEE Trans. on Commun.*, vol. 69, no. 7, pp. 4877–4889, July 2021.

[9] Q. Wu and R. Zhang, "Joint active and passive beamforming optimization for intelligent reflecting surface assisted SWIPT under QoS constraints," *IEEE J. Sel. Areas Commun.*, vol. 38, no. 8, pp. 1735–1748, Aug. 2020.

[10] Q. Wu and R. Zhang, "Intelligent reflecting surface enhanced wireless network via joint active and passive beamforming," *IEEE Trans. Wireless Commun.*, vol. 18, no. 11, pp. 5394–5409, Nov. 2019.

[11] Z. Chu, W. Hao, P. Xiao, D. Mi, Z. Liu, M. Khalily, J. R. Kelly, and A. P. Feresidis, "Secrecy rate optimization for intelligent reflecting surface assisted MIMO system," *IEEE Trans. Inf. Forensics Secur.*, vol. 16, pp. 1655–1669, 2021.

[12] Z. Zhang, C. Zhang, C. Jiang, F. Jia, J. Ge, and F. Gong, "Improving physical layer security for reconfigurable intelligent surface aided NOMA 6G networks," *IEEE Trans. Veh. Technol.*, vol. 70, no. 5, pp. 4451–4463, May 2021.

[13] H. Yang, Z. Xiong, J. Zhao, D. Niyato, L. Xiao, and Q. Wu, "Deep reinforcement learning-based intelligent reflecting surface for secure wireless communications," *IEEE Trans. Wireless Commun.*, vol. 20, no. 1, pp. 375–388, Jan. 2021.

[14] L. You, J. Xiong, D. W. K. Ng, C. Yuen, W. Wang, and X. Gao, "Energy efficiency and spectral efficiency tradeoff in RIS-aided multiuser MIMO uplink transmission," *IEEE Trans. Signal Process.*, vol. 69, pp. 1407–1421, Mar. 2021.

[15] A. Taha, M. Alrabeiah, and A. Alkhateeb, "Enabling large intelligent surfaces with compressive sensing and deep learning," *IEEE Access*, vol. 9, pp. 44 304–44 321, Mar. 2021.

[16] G. Zhou, C. Pan, H. Ren, K. Wang, and A. Nallanathan, "Intelligent reflecting surface aided multigroup multicast MISO communication systems," *IEEE Trans. Signal Process.*, vol. 68, pp. 3236–3251, Apr. 2020.

[17] H. Shen, W. Xu, S. Gong, Z. He, and C. Zhao, "Secrecy rate maximization for intelligent reflecting surface assisted multi-antenna communications," *IEEE Commun. Lett.*, vol. 23, no. 9, pp. 1488–1492, Sept. 2019.

[18] G. Zhou, C. Pan, H. Ren, K. Wang, M. Di Renzo, and A. Nallanathan, "Robust beamforming design for intelligent reflecting surface aided MISO communication systems," *IEEE Wireless commun. Lett.*, vol. 9, no. 10, pp. 1658–1662, Oct. 2020.

[19] S. Hong, C. Pan, H. Ren, K. Wang, K. K. Chai, and A. Nallanathan, "Robust transmission design for intelligent reflecting surface-aided secure communication systems with imperfect cascaded CSI," *IEEE Trans. Wireless Commun.*, vol. 20, no. 4, pp. 2487–2501, Apr. 2020.

[20] G. Zhou, C. Pan, H. Ren, K. Wang, and A. Nallanathan, "A framework of robust transmission design for IRS-aided MISO communications with

imperfect cascaded channels," *IEEE Trans. Signal Process.*, vol. 68, pp. 5092–5106, Aug. 2020.

[21] M. Badiu and J. P. Coon, "Communication through a large reflecting surface with phase errors," *IEEE Wireless Commun. Lett.*, vol. 9, no. 2, pp. 184–188, Feb. 2020.

[22] M. Jung, W. Saad, and G. Kong, "Spectral efficiency in large intelligent surfaces: Asymptotic analysis under pilot contamination," in *proc. IEEE GLOBECOM*, Dec. 2019, pp. 1–6.

[23] X. Yu, D. Xu, Y. Sun, D. W. K. Ng, and R. Schober, "Robust and secure wireless communications via intelligent reflecting surfaces," *IEEE J. Sel. Areas Commun.*, vol. 38, no. 11, pp. 2637–2652, Nov. 2020.

[24] A. A. Nasir, X. Zhou, S. Durrani, and R. A. Kennedy, "Relaying protocols for wireless energy harvesting and information processing," *IEEE Trans. Wireless Commun.*, vol. 12, no. 7, pp. 3622–3636, July 2013.

[25] Y. Zou, S. Gong, J. Xu, W. Cheng, D. T. Hoang, and T. D. Niyato, "Wireless powered intelligent reflecting surfaces for enhancing wireless communications," *IEEE Trans. Veh. Technol.*, vol. 69, no. 10, pp. 12 369–12 373, Oct. 2020.

[26] Z. Chu, P. Xiao, D. Mi, W. Hao, M. Khalily, and L.-L. Yang, "A novel transmission policy for intelligent reflecting surface assisted wireless powered sensor networks," *to apear in IEEE Sel. Top. Signal Process.*, 2021.

[27] B. Lyu, P. Ramezani, D. T. Hoang, S. Gong, Z. Yang, and A. Jamalipour, "Optimized energy and information relaying in self-sustainable IRS-empowered WPCN," *IEEE Trans. on Commun.*, vol. 69, no. 1, pp. 619–633, Jan. 2021.

[28] Y. Deng, Y. Zou, S. Gong, B. Lyu, D. T. Hoang, and D. Niyato, "Robust beamforming for IRS-assisted wireless communications under channel uncertainty," in *proc. IEEE WCNC*, Mar. 2021, pp. 1–6.

[29] M. M. Zhao, Q. Wu, M. J. Zhao, and R. Zhang, "Intelligent reflecting surface enhanced wireless network: two-timescale beamforming optimization," *IEEE Trans. Wireless Commun.*, vol. 20, no. 1, pp. 2–17, Jan. 2021.

[30] Q. Wu and R. Zhang, "Beamforming optimization for wireless network aided by intelligent reflecting surface with discrete phase shifts," *IEEE Trans. on Commun.*, vol. 68, no. 3, pp. 1838–1851, Mar. 2020.

[31] H. Yang, X. Chen, F. Yang, S. Xu, X. Cao, M. Li, and J. Gao, "Design of resistor-loaded reflectarray elements for both amplitude and phase control," *IEEE Antennas and Wirel. Propag. Lett.*, vol. 16, pp. 1159–1162, Nov. 2016.

[32] E. Boshkovska, D. W. K. Ng, N. Zlatanov, and R. Schober, "Practical non-linear energy harvesting model and resource allocation for SWIPT systems," *IEEE Commun. Lett.*, vol. 19, no. 12, pp. 2082–2085, Dec. 2015.

[33] Y. Zou, S. Gong, J. Xu, W. Cheng, D. T. Hoang, and D. Niyato, "Joint energy beamforming and optimization for intelligent reflecting surface enhanced communications," in *proc. IEEE WCNC Workshops*, May 2020, pp. 1–6.

[34] S. Boyd and L. Vandenberghe, *Convex optimization*. Cambridge, U.K.: Cambridge university press, 2004.

[35] Q. Wu and R. Zhang, "Intelligent reflecting surface enhanced wireless network: Joint active and passive beamforming design," in *proc. IEEE GLOBECOM*, Dec. 2018, pp. 1–6.

[36] B. Lyu, D. T. Hoang, S. Gong, D. Niyato, and D. I. Kim, "IRS-based wireless jamming attacks: When jammers can attack without power," *IEEE Wireless Commun. Lett.*, vol. 9, no. 10, pp. 1663–1667, Oct. 2020.

[37] M. Grant and S. Boyd, "CVX: Matlab software for disciplined convex programming, version 2.1," http://cvxr.com/cvx, 2018.

[38] Z. Luo, W. Ma, A. M. So, Y. Ye, and S. Zhang, "Semidefinite relaxation of quadratic optimization problems," *IEEE Signal Process. Mag.*, vol. 27, no. 3, pp. 20–34, May 2010.

[39] E. Delage and Y. Ye, "Distributionally robust optimization under moment uncertainty with application to data-driven problems," *Operations Research*, vol. 58, no. 3, pp. 595–612, Jan. 2010.

[40] G. D. Vita and G. Iannaccone, "Design criteria for the RF section of UHF and microwave passive RFID transponders," *IEEE Trans. Microw. Theory Techn.*, vol. 53, no. 9, pp. 2978–2990, Sept. 2005.

[41] Z.-Q. Luo, J. F. Sturm, and S. Zhang, "Multivariate nonnegative quadratic mappings," *SIAM Journal on Optimization*, vol. 14, no. 4, pp. 1140–1162, 2004.